# Fundamental bounds on qubit reset

Daniel Basilewitsch,[1,2] Jonas Fischer,[1,2,3] Daniel M. Reich,[1,2] Dominique Sugny,[3] and Christiane P. Koch[1,2,*]

[1]*Theoretische Physik, Universität Kassel, D-34132 Kassel, Germany*

[2]*Dahlem Center for Complex Quantum Systems and Fachbereich Physik, Freie Universität Berlin, Arnimallee 14, D-14195 Berlin, Germany*

[3]*Laboratoire Interdisciplinaire Carnot de Bourgogne (ICB), Université de Bourgogne-Franche Comté, F-21078 Dijon Cedex, France*

(Received 24 January 2020; accepted 25 January 2021; published 4 February 2021)

Qubit reset is a key task in the operation of quantum devices which, for many quantum hardware platforms, presently limits device clock speed. While it is known that coupling the qubit to an ancilla on demand allows for the fastest qubit reset, the limits on reset accuracy and speed due to the choice of ancilla have not yet been identified—despite the great flexibility in device design for most quantum hardware platforms. Here, we derive bounds on qubit reset in terms of maximum fidelity and minimum time, assuming control over the qubit and no control over the ancilla. For two-level ancillas, we find a provably time-optimal protocol which consists of purity exchange between qubit and ancilla brought into resonance. The globally minimal time can only be realized for specific choices of coupling and control which we identify. When increasing the size of the ancilla Hilbert space, the maximally achievable fidelity increases, whereas the reset time remains constant. Our results translate into device design principles for realizing, in a given quantum architecture, the fastest and most accurate protocol for qubit reset.

DOI: 10.1103/PhysRevResearch.3.013110

## I. INTRODUCTION

The ability to initialize qubits from an arbitrary mixed state to a fiducial pure state is a basic building block in quantum information (QI) science [1]. Initializing the qubit or, equivalently, resetting it after completion of a computational task, requires some means to export entropy. At the same time, for device operation, the qubit needs to be well-protected and isolated from its environment. It is thus not an option to simply let the qubit equilibrate with its environment; rather, active reset is indispensable. A common approach to actively initialize a qubit uses projective measurements [2] but, for many QI architectures, this suffers from being slow, see, e.g., Refs. [3,4] for the example of superconducting qubits. Rapid reset is made possible by coupling each qubit to an ancilla in a tunable way. This can be a fast decaying state, such as in laser cooling, or an auxiliary system such as another qubit [5,6] or a resonator [7–9]. Then, the coupling strength together with either the switching time for the coupling or the ancilla decay rate determine the overall time required to reset the qubit. This bound on the reset protocol duration is a specific instance of open quantum system speed limits [10]. At present, the overall time required for qubit reset presents one of the main limitations for device operation, especially for superconducting qubits. On the other hand, in these architectures, there exists a great flexibility in the design of tunable couplings between qubit and ancilla [11], a flexibility that could be used to improve the speed and accuracy of qubit reset.

Here, we derive bounds on reset accuracy and speed, assuming no external control over the ancilla, and identify device designs, in terms of the types of interaction and control, that allow for attaining the bounds. Starting with a two-level ancilla, where the reset dynamics is an element of SU(4), we can leverage earlier results on the quantum optimal control in SU(4) [12–15] for qubit reset. Making use of the Cartan decomposition of SU(4) [16,17], we identify the qubit-ancilla couplings which allow for qubit purification. For all Hamiltonians fulfilling this criterion, we use quantum optimal control theory [18] to determine the controls on the qubit that realize a time-optimal reset. Moreover, we identify the dynamics for maximum purity reset when the ancilla Hilbert space dimension is larger than two. A combination of geometric, algebraic, and numerical tools allows us to identify ultimate performance limits for duration and accuracy of qubit reset.

Our focus on using an ancilla to reset the qubit is motivated by the fact that weakly coupled environmental modes cannot be harnessed for time-optimal reset [6,19]. The ancilla can be realized by a strongly coupled environmental mode [20,21] but also by another engineered quantum system [8,22–24]. In that scenario, both qubit and ancilla are weakly coupled to the larger thermal environment, which allows the ancilla to equilibrate after being decoupled from the qubit.

## II. RESET WITH A TWO-LEVEL ANCILLA

We first consider a two-level ancilla and identify the necessary conditions on the qubit-ancilla time evolution operator $\mathsf{U}$ to allow for purification of the qubit. Employing the Cartan

*christiane.koch@fu-berlin.de

decomposition of SU(4), every element $\mathsf{U} \in \mathrm{SU}(4)$ can be written as [25]

$$\mathsf{U} = \mathsf{K}\mathsf{A}\mathsf{K}', \quad \mathsf{A} = \exp\left\{\frac{\mathrm{i}}{2}\sum_{k=1}^{3} c_k(\sigma_k \otimes \sigma_k)\right\}, \tag{1}$$

with $\mathsf{K}, \mathsf{K}' \in \mathrm{SU}(2) \otimes \mathrm{SU}(2)$ and $\sigma_k$ the usual Pauli matrices. This representation allows one to separate the evolution operator $\mathsf{U}$ into local ($\mathsf{K}$, $\mathsf{K}'$) and nonlocal (NL) ($\mathsf{A}$) parts. In the following, we refer to the coefficients $c_k \in [0, \pi]$ as NL coordinates and, for convenience, write $\mathsf{K} = \mathsf{k}_\mathrm{S} \otimes \mathsf{k}_\mathrm{B}$ where $\mathsf{k}_\mathrm{S}$ and $\mathsf{k}_\mathrm{B}$ are local operations on qubit and ancilla (denoted by subscripts S and B for system and bath). Assuming the joint initial state to be separable, $\rho(0) = \rho_\mathrm{S}(0) \otimes \rho_\mathrm{B}(0)$, the qubit state at time $t$ is given by

$$\rho_\mathrm{S}(t) = \mathrm{tr}_\mathrm{B}\{\mathsf{U}(t)\rho(0)\mathsf{U}^\dagger(t)\} = \mathcal{D}_{\rho_\mathrm{B}(0)}(t)[\rho_\mathrm{S}(0)], \tag{2}$$

where the dynamical map of the qubit, $\mathcal{D}_{\rho_\mathrm{B}(0)}$, depends parametrically on the initial ancilla state, $\rho_\mathrm{B}(0)$. A necessary condition for purification of a quantum system is nonunitality [26] of its dynamical map [27]. To check unitality in Eq. (2), we consider the initial state

$$\rho(0) = \mathbb{1}_\mathrm{S} \otimes \rho_\mathrm{B}(0), \quad \rho_\mathrm{B}(0) = \begin{pmatrix} p_\mathrm{B}^\mathrm{e} & \gamma_\mathrm{B} \\ \gamma_\mathrm{B}^* & p_\mathrm{B}^\mathrm{g} \end{pmatrix}, \tag{3}$$

where $p_\mathrm{B}^\mathrm{g}, p_\mathrm{B}^\mathrm{e} \in [0, 1]$ denote the ancilla ground and excited state populations, and $\gamma_\mathrm{B} \in \mathbb{C}$ its coherence. Using Eqs. (1), we find

$$\begin{aligned}\mathcal{D}_{\rho_\mathrm{B}(0)}[\mathbb{1}_\mathrm{S}] &= \mathrm{tr}_\mathrm{B}\{\mathsf{U}(\mathbb{1}_\mathrm{S} \otimes \rho_\mathrm{B}(0))\mathsf{U}^\dagger\} \\ &= \mathsf{k}_\mathrm{S}\mathrm{tr}_\mathrm{B}\{\mathsf{A}(\mathbb{1}_\mathrm{S} \otimes \rho_\mathrm{B}')\mathsf{A}^\dagger\}\mathsf{k}_\mathrm{S}^\dagger,\end{aligned} \tag{4}$$

where

$$\rho_\mathrm{B}' = \mathsf{k}_\mathrm{B}'\rho_\mathrm{B}(0)\mathsf{k}_\mathrm{B}'^\dagger = \begin{pmatrix} p_\mathrm{B}^{\mathrm{e}\prime} & \gamma_\mathrm{B}' \\ \gamma_\mathrm{B}'^* & p_\mathrm{B}^{\mathrm{g}\prime} \end{pmatrix}$$

is the locally transformed ancilla state. Unitality of $\mathcal{D}_{\rho_\mathrm{B}(0)}$ is determined by the partial trace in Eq. (4) since $\mathsf{k}_\mathrm{S}\mathbb{1}_\mathrm{S}\mathsf{k}_\mathrm{S}^\dagger = \mathbb{1}_\mathrm{S}$ for any $\mathsf{k}_\mathrm{S}$. The partial trace yields

$$\begin{aligned}\mathrm{tr}_\mathrm{B}\{\mathsf{A}(\mathbb{1}_\mathrm{S} \otimes \rho_\mathrm{B}')\mathsf{A}^\dagger\} = \mathbb{1}_\mathrm{S} &+ 2\Re\mathrm{e}(\gamma_\mathrm{B}')\sin(c_2)\sin(c_3)\sigma_1 \\ &- 2\Im\mathrm{m}(\gamma_\mathrm{B}')\sin(c_1)\sin(c_3)\sigma_2 \\ &- \left(p_\mathrm{B}^{\mathrm{g}\prime} - p_\mathrm{B}^{\mathrm{e}\prime}\right)\sin(c_1)\sin(c_2)\sigma_3.\end{aligned} \tag{5}$$

Equation (5) implies that any $\mathsf{U} \in \mathrm{SU}(4)$ with only a single nonvanishing $c_k$ yields a unital map for the qubit and purification is not possible at all. Occurrence of two nonvanishing NL coordinates is necessary but not yet sufficient for nonunitality of $\mathcal{D}_{\rho_\mathrm{B}(0)}$ due to the dependence on $\rho_\mathrm{B}'$, i.e., on the initial ancilla state $\rho_\mathrm{B}(0)$ and local operation $\mathsf{k}_\mathrm{B}'$. Nonunitality of $\mathcal{D}_{\rho_\mathrm{B}(0)}$, independent of the ancilla, is guaranteed by three nonvanishing NL coordinates [28].

With this observation, we can relate nonunitality of $\mathcal{D}_{\rho_\mathrm{B}(0)}$ with the entangling capability of $\mathsf{U}$ for the qubit-ancilla system. The latter is best analyzed in the Weyl chamber [25], which is a symmetry-reduced version of the cube spanned by $c_1, c_2, c_3 \in [0, \pi]$, obtained when eliminating redundancies in Eqs. (1). The six symmetries are sketched in the upper part of Fig. 1 with the Weyl chamber shown below. The shaded

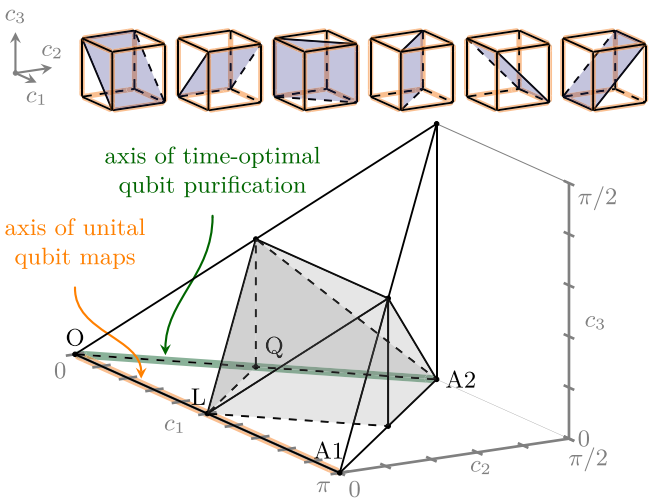


FIG. 1. (Color online.) Symmetries (upper part) and construction of the Weyl chamber (lower part) for the characterization of the nonlocal content of any two-qubit operation $\mathsf{U} \in \mathrm{SU}(4)$, cf. Eqs. (1). The shaded polyhedron within the Weyl chamber describes all perfectly entangling operations. The orange line highlights those $\mathsf{U}$ which lead to unital maps for the qubit. The green line anticipates a time-optimal path for qubit purification identified below. The letters mark specific elements of SU(4) referred to in the text.

polyhedron in its center describes all perfectly entangling operations and the $c_1$ axis represents all operations with at most one nonvanishing NL coordinate. It contains one point of the polyhedron of perfect entanglers—the point L corresponding to the gate cNOT and all gates that are locally equivalent to it, including cPHASE. Albeit being perfect entanglers, cNOT and cPHASE yield unital maps for the qubit. The capability of $\mathsf{U}$ to create entanglement between qubit and ancilla is thus a necessary but not sufficient condition for purification of the qubit.

Next, we determine the qubit-ancilla couplings that allow for purification of the qubit. To this end, we write the generic qubit-ancilla Hamiltonian,

$$\mathsf{H}(t) = \mathsf{H}_\mathrm{S}(t) \otimes \mathbb{1}_\mathrm{B} + \mathbb{1}_\mathrm{S} \otimes \mathsf{H}_\mathrm{B} + \mathsf{H}_\mathrm{int}, \tag{6}$$

with $\mathsf{H}_\mathrm{S}(t) = \frac{\omega_\mathrm{S}}{2}\sigma_3 + \mathcal{E}(t)\mathsf{O}_\mathrm{c}$, $\mathsf{H}_\mathrm{B} = \frac{\omega_\mathrm{B}}{2}\sigma_3$, and $\mathsf{H}_\mathrm{int} = J(\mathsf{O}_\mathrm{S} \otimes \mathsf{O}_\mathrm{B})$, assuming control, via an external field $\mathcal{E}(t)$, only over the qubit. $J$ denotes the qubit-ancilla coupling strength [29], while $\omega_\mathrm{S} < \omega_\mathrm{B}$ are the level splittings of qubit and ancilla. For simplicity, we start by taking the operators to be Pauli matrices, $\mathsf{O}_\mathrm{S}, \mathsf{O}_\mathrm{B}, \mathsf{O}_\mathrm{c} \in \{\sigma_1, \sigma_2, \sigma_3\}$, and show later that our results also hold for superpositions of Pauli operators. To relate the Hamiltonian Eq. (6) to the purification condition, which is stated in terms of the number $N_\mathrm{c}$ of nonzero NL coordinates of the joint qubit-ancilla time evolution, we consider the dynamical Lie algebra $\mathcal{L}$. Its Cartan decomposition, $\mathcal{L} = \mathfrak{k} \oplus \mathfrak{p}$, implies that $\mathsf{A}$ in Eqs. (1) is an element of the group $\exp\{\mathfrak{a}\}$ where $\mathfrak{a}$ is the Cartan subalgebra, i.e., the maximal Abelian subalgebra of $\mathfrak{p}$. For Hamiltonian Eq. (6) and the control task of purifying the qubit, it turns out that $N_\mathrm{c} = \dim\{\mathfrak{a}\}$ [30]. Since $\mathfrak{a}$ can be determined entirely from the Hamiltonian, without any knowledge of the actual dynamics, $N_\mathrm{c}$ is readily obtained. It is thus straightforward

to identify the combinations $\mathsf{O}_S, \mathsf{O}_B, \mathsf{O}_c \in \{\sigma_1, \sigma_2, \sigma_3\}$ for which $N_c \geqslant 2$: Out of the $3 \times 3 \times 3$ possible combinations of $\mathsf{O}_S, \mathsf{O}_B, \mathsf{O}_c$, only 16 have a Cartan subalgebra $\mathfrak{a}$ of dimension 2, allowing for purification of the qubit [31]. Table II in the Appendix summarizes the resulting dynamical Lie algebras and presents possible choices for $\mathfrak{a}$.

After identifying the cases in which Hamiltonian Eq. (6) allows for purification of the qubit, we seek to derive the fields $\mathcal{E}(t)$ which reset the qubit in minimum time. This requires consideration not only of the generators but also of the full dynamics. We assume a separable initial state with the ancilla in thermal equilibrium, i.e., without ancilla coherence:

$$\rho(0) = \begin{pmatrix} p_S^e & \gamma_S \\ \gamma_S^* & p_S^g \end{pmatrix} \otimes \begin{pmatrix} p_B^e & 0 \\ 0 & p_B^g \end{pmatrix}. \tag{7}$$

Before stating the general result, we present three observations based on numerical simulations of all 16 cases. (i) For a constant resonant field, the minimum time, $T_{\min}$, to achieve maximal qubit purity is independent of the initial qubit state, $\rho_S(0)$. Such a field puts qubit and ancilla into resonance, i.e., $\mathcal{E}$ is chosen such that $\lambda_1 - \lambda_0 = \omega_B$ where $\lambda_0 < \lambda_1$ are the field-dressed eigenvalues of the qubit Hamiltonian $\mathsf{H}_S$. This generalizes the results of Ref. [6] to the remaining 15 cases where purification is possible. (ii) The specific value of $T_{\min}$ depends on the type of qubit-ancilla interaction and local control, i.e., on the choice of $\mathsf{O}_S$, $\mathsf{O}_B$, $\mathsf{O}_c$. (iii) When allowing for fully time-dependent control fields $\mathcal{E}(t)$, the maximal qubit purity cannot be reached faster than $T_{\min}$. However, for times $\tau < T_{\min}$, numerical optimizations using Krotov's method [32,33] lead to an upper bound for the qubit purity $\mathcal{P}_S(\tau)$, given in terms of the evolution of the thermal initial state $\rho_S(0)$ under resonant fields. The optimally shaped fields saturating the bound depend both on the initial state and the choice of $\mathsf{O}_S, \mathsf{O}_B, \mathsf{O}_c$.

We discuss these observations in more detail for $\mathsf{O}_S = \mathsf{O}_B = \sigma_1$ with (a) $\mathsf{O}_c = \sigma_1$ and (b) $\mathsf{O}_c = \sigma_3$, cf. Fig. 2. These two examples are paradigmatic, with all other combinations of $\mathsf{O}_S$, $\mathsf{O}_B$, and $\mathsf{O}_c$ yielding identical results (data not shown). In case (b), we know that time-optimal reset is achieved with a constant field $\mathcal{E}(t) = \mathcal{E}$ that puts qubit and ancilla into resonance [6]. A constant resonant field therefore seems to be a suitable pilot for all numerical optimizations. For all initial states of the qubit (randomly chosen under the condition of identical purity), a maximum in the time evolution of the purity occurs at roughly the same point in time, $T_{\min}$, when applying the constant resonant field, cf. Fig. 2. Using optimal control theory, we find field shapes $\mathcal{E}(t)$, $t \in [0, \tau]$ that maximize $\mathcal{P}_S(\tau)$ at a given time $\tau$. For a few choices of $\tau$, the black and red dots in Fig. 2 compare the purities obtained with constant resonant and optimized fields [34]. In all cases with $\tau \neq T_{\min}$, the optimized fields improve the purity compared to the constant resonant field. For $\tau = T_{\min}$, the purities coincide (since the constant resonant field is already an optimal solution). For $\tau < T_{\min}$, there exists an upper bound for $\mathcal{P}_S(\tau)$, which is attained by the constant resonant field for a coherence-free initial qubit state with $p_S^g > p_S^e$. This bound can be proven rigorously, see, e.g., Ref. [22] and Appendix A 2. While the individual optimized fields depend on $\tau$ and, for $\tau \neq T_{\min}$, also on the initial state of the qubit, they

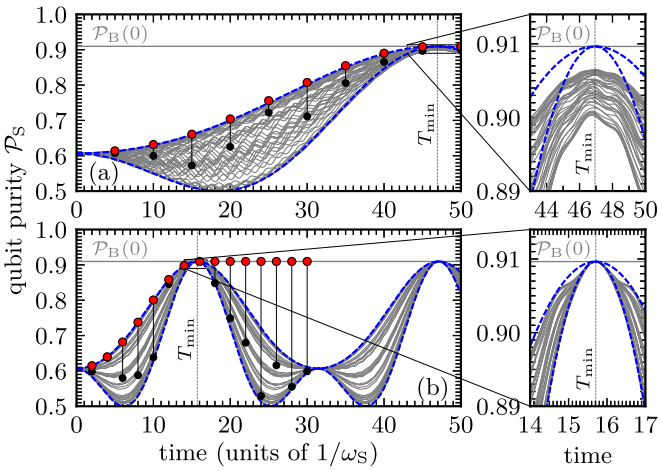


FIG. 2. (Color online.) The time evolution of the qubit purity reveals the minimum time for qubit reset—shown here for the examples $\mathsf{H}_{\text{int}} = J(\sigma_1 \otimes \sigma_1)$ with $\mathsf{H}_c(t) = \mathcal{E}(t)\,\sigma_1$ (a) and $\mathsf{H}_c(t) = \mathcal{E}(t)\,\sigma_3$ (b). The gray area corresponds to the superimposed evolutions of 50 different initial states $\rho(0) = \rho_S(0) \otimes \rho_B(0)$ with $\rho_B(0)$ the thermal equilibrium state and $\rho_S(0)$ sampled randomly under the condition of identical purity. The red (black) dots indicate the values for $\mathcal{P}_S(\tau)$ obtained with optimized (constant resonant) $\mathcal{E}(t)$. The dashed blue lines indicate the upper and lower bounds of $\mathcal{P}_S$ predicted by Eq. (8). $\mathcal{P}_B(0)$ denotes the initial ancilla purity. The parameters are $\omega_S = 1$, $\omega_B = 3$, $J = 0.1$, and inverse temperature $\beta = 1$.

all exhibit a strong off-resonant initial peak which, if $\gamma_S \neq 0$, rotates the coherence into population or, if $p_S^g < p_S^e$, inverts the qubit populations, before swapping the purities with the resonant protocol [6]. When allowing for times $\tau > T_{\min}$, a purity swap between qubit and ancilla remains the optimal strategy, with the corresponding fields being more complex than the constant resonant solution for $\tau = T_{\min}$.

Based on these numerical results, we conjecture that time-optimal purification requires one to choose a constant and resonant field, $\mathcal{E}(t) = \mathcal{E}$, such that $\lambda_1 - \lambda_0 = \omega_B$, no matter what the choice is of $\mathsf{O}_S$, $\mathsf{O}_B$, or $\mathsf{O}_c$. For a constant and resonant $\mathcal{E}(t)$, an exact closed-form expression for the joint time evolution operator can be approximated to yield an expression for the time evolution of the qubit purity, cf. Eq. (A15). For the example of case (a), it reads

$$\begin{aligned} \mathcal{P}_S(t) \approx & \left[p_S^g p_B^g + p_S^g p_B^e \cos^2(\eta t) + p_S^e p_B^g \sin^2(\eta t)\right]^2 \\ & + \left[p_S^e p_B^e + p_S^g p_B^e \sin^2(\eta t) + p_S^e p_B^g \cos^2(\eta t)\right]^2 \\ & + 2|\gamma_S|^2 \cos^2(\eta t), \end{aligned} \tag{8}$$

with

$$\eta^2 = J^2 + \frac{\omega_B}{2}\left(\omega_B - \sqrt{\omega_B^2 + 4B^2}\right), \quad B^2 = J^2 \frac{\omega_B^2 - \omega_S^2}{\omega_B^2}. \tag{9}$$

Here, $\eta$ denotes the effective coupling strength, the value of which depends on the choice of $\mathsf{O}_S$, $\mathsf{O}_B$, and $\mathsf{O}_c$. Maximizing $\mathcal{P}_S(t)$ yields an approximated minimum time for purification, $T_{\min} = \pi/(2\eta)$, independent of the initial state. This explains why $\mathcal{P}_S(t)$ displays a perfect swap of qubit and ancilla purity at $T_{\min}$ for all evolutions in Fig. 2(a). For all other Hamiltonians which allow for purification, we obtain the same result

TABLE I. Minimum reset times $T_{\min}^{(i)}$ for two coupled superconducting qubits [35] with three sets of experimental parameters (set 1: $\omega_S/(2\pi) = 12.8$ GHz, $\omega_B/(2\pi) = 16.1$ GHz, $J/(2\pi) = 65$ MHz; set 2: $\omega_S/(2\pi) = 9.8$ GHz, $\omega_B/(2\pi) = 16.1$ GHz, $J/(2\pi) = 200$ MHz; set 3: $\omega_S/(2\pi) = 15.8$ GHz, $\omega_B/(2\pi) = 16.1$ GHz, $J/(2\pi) = 25$ MHz [36]). The choice of $\mathsf{O}_S, \mathsf{O}_B, \mathsf{O}_c$ determines the type $(i)$ of the minimal time $T_{\min}^{(i)}$ in Eqs. (10) with $(i)$ indicated in the last column.

| $\mathsf{O}_S \otimes \mathsf{O}_B$ | $\mathsf{O}_c$ | $T_{\min}^{(i)}$ (set 1) | $T_{\min}^{(i)}$ (set 2) | $T_{\min}^{(i)}$ (set 3) | $(i)$ |
|---|---|---|---|---|---|
| $\sigma_1 \otimes \sigma_1$ | $\sigma_1$ | 191.0 ns | 81.1 ns | 402.3 ns | (2) |
| $\sigma_1 \otimes \sigma_1$ | $\sigma_2$ | 151.8 ns | 49.3 ns | 394.8 ns | (1) |
| $\sigma_1 \otimes \sigma_1$ | $\sigma_3$ | 151.8 ns | 49.3 ns | 394.8 ns | (1) |
| $\sigma_1 \otimes \sigma_2$ | $\sigma_1$ | 191.0 ns | 81.1 ns | 402.3 ns | (2) |
| $\sigma_1 \otimes \sigma_2$ | $\sigma_2$ | 151.8 ns | 49.3 ns | 394.8 ns | (1) |
| $\sigma_1 \otimes \sigma_2$ | $\sigma_3$ | 151.8 ns | 49.3 ns | 394.8 ns | (1) |
| $\sigma_2 \otimes \sigma_1$ | $\sigma_1$ | 151.8 ns | 49.3 ns | 394.8 ns | (1) |
| $\sigma_2 \otimes \sigma_1$ | $\sigma_2$ | 191.0 ns | 81.1 ns | 402.3 ns | (2) |
| $\sigma_2 \otimes \sigma_1$ | $\sigma_3$ | 151.8 ns | 49.3 ns | 394.8 ns | (1) |
| $\sigma_2 \otimes \sigma_2$ | $\sigma_1$ | 151.8 ns | 49.3 ns | 394.8 ns | (1) |
| $\sigma_2 \otimes \sigma_2$ | $\sigma_2$ | 191.0 ns | 81.1 ns | 402.3 ns | (2) |
| $\sigma_2 \otimes \sigma_2$ | $\sigma_3$ | 151.8 ns | 49.3 ns | 394.8 ns | (1) |
| $\sigma_3 \otimes \sigma_1$ | $\sigma_1$ | 250.3 ns | 62.2 ns | 2054.6 ns | (3) |
| $\sigma_3 \otimes \sigma_1$ | $\sigma_2$ | 250.3 ns | 62.2 ns | 2054.6 ns | (3) |
| $\sigma_3 \otimes \sigma_2$ | $\sigma_1$ | 250.3 ns | 62.2 ns | 2054.6 ns | (3) |
| $\sigma_3 \otimes \sigma_2$ | $\sigma_2$ | 250.3 ns | 62.2 ns | 2054.6 ns | (3) |

for $\mathcal{P}_S(t)$, Eq. (8), but with different expressions for effective coupling $\eta$ and and the parameter $B$, cf. Appendix A 2. For example, in case (b) $B = 0$ and hence $\eta = J$ leads to $T_{\min} = \pi/(2J)$, which is much shorter than $T_{\min}$ in case (a) where $B \neq 0$, cf. Fig. 2.

Overall, we find three distinct minimal reset times which can be linked to a single quantity $A$ such that $T_{\min} \approx \pi/(2|A|)$. For all possible combinations of $\mathsf{O}_S, \mathsf{O}_B, \mathsf{O}_c \in \{\sigma_1, \sigma_2, \sigma_3\}$, $A$ is obtained directly from the Hamiltonian and determined by the parameters $J$, $\omega_S$, and $\omega_B$, cf. Eq. (A18) and Table III. Depending on the choice of $\mathsf{O}_S, \mathsf{O}_B, \mathsf{O}_c$, the minimal times are

$$T_{\min}^{(1)} = \frac{\pi}{2J}, \quad T_{\min}^{(2)} = \frac{\pi}{2J}\frac{\omega_B}{\omega_S}, \quad T_{\min}^{(3)} = \frac{\pi}{2J}\frac{\omega_B}{\sqrt{\omega_B^2 - \omega_S^2}}, \tag{10}$$

see also Table I. Note that $T_{\min}^{(3)}$ approaches $T_{\min}^{(1)}$ for $\omega_B \gg \omega_S$ (recall that $\omega_B > \omega_S$ for reset). Inspection of Table I reveals which operator combinations give rise to the three cases, allowing us to rationalize why $T_{\min}^{(1)}$ represents the shortest time among the three cases. First, the choice $\mathsf{O}_S = \sigma_3$ is not expected to be optimal for a protocol based on purity exchange. In this case, an exchange interaction is generated by commutators of $\mathsf{H}_{\text{int}}$ and $\mathsf{O}_c \otimes \mathbb{1}_B$, but not by $\mathsf{H}_{\text{int}}$ itself. The commutators occur only in higher order terms of a series expansion of the time evolution operator, i.e., they require more time to become effective. Next, if $\mathsf{O}_S \otimes \mathsf{O}_B$ are chosen to directly implement an exchange interaction, the fastest reset [cf. case (1) in Table I] is obtained if $\mathsf{O}_c$ does not commute with $\mathsf{O}_S$. More precisely, the norm of $[\mathsf{O}_S, \mathsf{O}_c]$ can be related to the rate of heat exchange between qubit and ancilla, as we show in Appendix A 3.

When allowing $\mathsf{O}_S$, $\mathsf{O}_B$, and $\mathsf{O}_c$ to be arbitrary elements of $\mathfrak{su}(2) = \text{span}\{\sigma_1, \sigma_2, \sigma_3\}$ including superpositions of Pauli operators, we still find the respective minimum times for the purity swap to be lower bounded by $T_{\min}^{(1)}$. Our proof makes use of the time-optimal tori theorem for SU(4) [12], the details of which are presented in Appendix A 1. Here, we briefly highlight the major points. The time-optimal tori theorem derives a lower bound on the time to realize an arbitrary unitary $\mathsf{U} \in \text{SU}(4)$ of the form Eqs. (1). To this end, full controllability is assumed, i.e., controls can, unlike in our setting, also act on the ancilla. As a result, any local operation $\mathsf{K}, \mathsf{K}' \in \text{SU}(2) \otimes \text{SU}(2)$ can be generated. Under these conditions, the minimal time to realize an arbitary $\mathsf{U} \in \text{SU}(4)$ is determined by the NL part $\mathsf{A}$ of $\mathsf{U}$. Accounting for the nonuniqueness of the NL coordinates $c_k$, it is given by the smallest possible value of $T_{\min} = \sum_k \frac{c_k}{2J}$. In view of qubit reset, we are interested in a specific unitary, namely, the one that maximizes the qubit purity when starting from a completely mixed state, $\rho_S(0) = \mathbb{1}_S/2$. In other words, we need to find those NL coordinates $c_k$ that not only minimize $T_{\min} = \sum_k \frac{c_k}{2J}$ but also maximize

$$\begin{aligned}\mathcal{P}_S &= \text{tr}\left\{\text{tr}_B^2\left\{\mathsf{A}\left(\frac{\mathbb{1}_S}{2} \otimes \rho_B'\right)\mathsf{A}^\dagger\right\}\right\} \\ &= \frac{1}{2} + \left((p_B^{g'})^2 + (p_B^{e'})^2 - \frac{1}{2}\right)\sin^2(c_1)\sin^2(c_2) \\ &\quad + 2\,\mathfrak{Re}(\gamma_B')^2 \sin^2(c_2)\sin^2(c_3) \\ &\quad + 2\,\mathfrak{Im}(\gamma_B')^2 \sin^2(c_1)\sin^2(c_3),\end{aligned} \tag{11}$$

where we have used Eq. (5). We find maxima of the qubit purity $\mathcal{P}_S$ in Eq. (11) if two of the $c_k$ are equal to $\pi/2$ while the third one vanishes. This results in a global minimum for the reset time, $T_{\min} = \pi/(2J)$. Remarkably, the global minimum coincides with the minimal reset time $T_{\min}^{(1)}$ that we have identified above under the assumption of control over the qubit but not the ancilla.

Table I shows exemplary minimum reset times $T_{\min}$ for a physical realization of two coupled superconducting qubits [35,36], illustrating the role of device design in terms of the choice of $\mathsf{O}_S$, $\mathsf{O}_B$, and $\mathsf{O}_c$ as well as the parameters $\omega_S$, $\omega_B$, and $J$. In case of the optimal choice of $\mathsf{O}_S$, $\mathsf{O}_B$, and $\mathsf{O}_c$ such that $T_{\min} = T_{\min}^{(1)}$ (independently of $\omega_B$), $\omega_B$ should still be chosen as large as possible to increase the maximum achievable purity. An option to effectively enlarge $\omega_B$ is to utilize ancilla levels above the two-level subspace. This raises the question whether our findings on minimum protocol duration and maximum reset fidelity also hold for ancillas with Hilbert space dimension larger than two.

## III. RESET WITH A MULTILEVEL ANCILLA

We now inspect ancillas with Hilbert space dimension $d > 2$ since most quantum systems that can act as ancilla intrinsically possess more than two levels. Here, we explore whether additional levels, energetically above the ground and first excited state, are potentially beneficial for fast on-demand

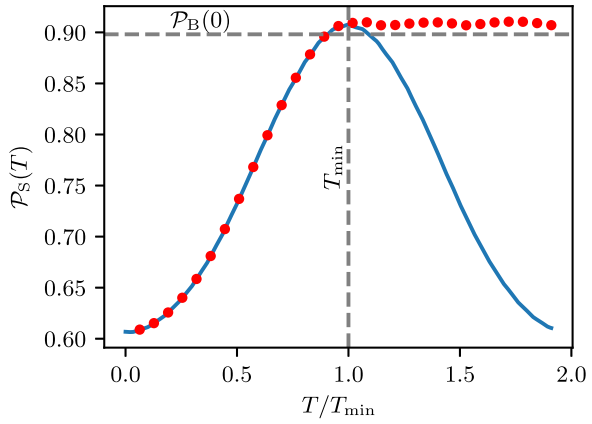


FIG. 3. Purity evolution of a qubit interacting with a qutrit ancilla under a constant, resonant field (blue line). The resonance condition is set with respect to the $|0\rangle \leftrightarrow |1\rangle$ transition in the qutrit, as these are the initially most populated levels. With numerically optimized fields, we also obtained the maximal purity for specific times (red dots). Parameters as in Fig. 2 and $\omega_{B,1} = 3$ and $\omega_{B,2} = 2$.

reset. We discuss both aspects of reset, i.e., the minimal reset time as well as the maximal achievable qubit purity.

To investigate whether an increase of the Hilbert space dimension $d$ of the ancilla allows for faster purification, we first choose the ancilla to be a qutrit ($d = 3$). In the following, we focus on a local $\sigma_3$ control on the qubit and generalize the previously discussed $\sigma_1 \otimes \sigma_1$ qubit-ancilla-interaction, cf. Fig. 2, which for two-level ancillas yields the globally minimal purification time $T_{min} = \pi/(2J)$, to the qubit-qutrit case. To this end, we write the interaction Hamiltonian as $\mathsf{H}_{int} = J[\sigma_1 \otimes (\mathsf{a} + \mathsf{a}^\dagger)]$, where $\mathsf{a}$ and $\mathsf{a}^\dagger$ are the truncated lowering and raising operators, respectively. The ancilla (or bath) Hamiltonian is given by $\mathsf{H}_B = \mathrm{diag}\{\omega_{B,2}, 0, -\omega_{B,1}\}$, with $\omega_{B,1}$ and $\omega_{B,2}$ the transition frequencies between the qutrit's ground and first excited state, respectively, first and second excited state. As before, we assume uncorrelated initial thermal states on the system and ancilla.

To examine a possible change in the minimal reset time due to the addition of a third level, we have numerically maximized the qubit purity for different final times $T$, cf. Fig. 3. The highest purity in Fig. 3 is observed for times equal or larger than $T_{min}$, i.e., the minimum time to achieve maximum purity is identical to the case of a two-level ancilla. Analogous simulations for $d = 4$ (data not shown) yield the same minimum purification time. We therefore conjecture that $T_{min}$ is independent of the ancilla Hilbert space dimension.

Moreover, we observe that, for all $T < T_{min}$ in Fig. 3, a resonant guess field (blue line) yields the maximally achievable qubit purity, where the resonance is taken with respect to $\omega_{B,1}$. We therefore conjecture, based on numerical evidence, that resonant fields also remain an optimal reset strategy for ancillas with Hilbert space dimension $d > 2$.

Figure 3 allows for another important observation: While the minimum reset time $T_{min}$ is unchanged for $d = 3$ compared to $d = 2$, the maximal achievable purity increases, cf. the red dots and dashed horizontal line which corresponds to the maximal qubit purity in case of a two-level ancilla. Remarkably, the maximal achievable qubit purity is no longer upper bounded by the initial ancilla purity, $\mathcal{P}_B(0)$. This raises the question whether the maximal qubit purity can be further enhanced by allowing for even larger $d$. We will answer this question in its most general form, i.e., considering a system and ancilla with Hilbert space dimensions $d_S$ and dimension $d_B$, respectively. The following proposition links the maximal achievable system purity to the ancilla dimension $d_B$ and its initial state.

*Proposition 1.* Let $\mathcal{H}_S$ and $\mathcal{H}_B$ be Hilbert spaces with dimensions $d_S$ and $d_B$, respectively, and $\mathfrak{L}_{\mathcal{H}_S}$ and $\mathfrak{L}_{\mathcal{H}_B}$ their corresponding Liouville spaces. Let $\rho_B \in \mathfrak{L}_{\mathcal{H}_B}$ be a density matrix with at least $\lceil d_B(d_S - 1)/d_S \rceil$ eigenvalues below $\epsilon/[2d_B(d_S - 1)]$ with small $\epsilon > 0$, where $\lceil \cdot \rceil$ denotes the ceiling function. Then, for all density matrices $\rho_S \in \mathfrak{L}_{\mathcal{H}_S}$, there exists a $\mathsf{U} \in \mathrm{SU}(d_S d_B)$ such that

$$1 - \mathrm{tr}\{\rho_S'^2\} \leqslant \epsilon, \quad \rho_S' = \mathrm{tr}_B\{\mathsf{U}(\rho_S \otimes \rho_B)\mathsf{U}^\dagger\}, \tag{12}$$

i.e., the purity of $\rho_S'$ gets $\epsilon$-close to unity.

While the technical details and proof of this proposition are discussed in Appendix B, here we focus on the interesting physical implications of this proposition. To this end, let us consider the requirements for the perfect purification of a qubit, i.e., $d_S = 2$ and $\epsilon = 0$, by an ancilla with Hilbert space dimension $d_B$. For the special case of a two-level ancilla, as discussed earlier, we find $\lceil d_B(d_S - 1)/d_S \rceil = \lceil 2(2-1)/2 \rceil = 1$. According to Proposition 1, this implies that the initial ancilla state $\rho_B$ needs to have one vanishing eigenvalue for the final qubit state $\rho_S'$ to become pure. In other words, perfect purification of the qubit is only possible with initially pure ancillas. For $d_B = 3$, we find $\lceil d_B/2 \rceil = 2$, which means that we still require a pure initial ancilla state for successful purification of the qubit. However, starting from $d_B = 4$, it is possible to fully purify the qubit even if more than one eigenvalue of $\rho_B$ is large. In other words, for $d_B \geqslant 4$, the initial ancilla state $\rho_B$ does not need to be pure for perfect purification.

Proposition 1 furthermore implies that even if perfect purification of the system is not possible, the system can still be purified beyond a simple swap of purities as long as $d_B > 2$ holds. To illustrate this, let us again consider the purification of a qubit ($\omega_S = 1$) and let us assume an ancilla with equidistant energy levels ($\omega_S = 3$). We assume thermal initial states with inverse thermal energy $\beta = 1$ on both qubit and ancilla. In this scenario, starting again with $d_B = 2$, the maximally achievable qubit purity is $\mathcal{P}_S^{max} \approx 0.905$, which amounts exactly to a swap of purities as observed earlier. In contrast, for $d_B = 3$ and $d_B = 4$, we find $\mathcal{P}_S^{max} \approx 0.970$ and $\mathcal{P}_S^{max} \approx 0.995$, respectively, which illustrates the potential improvement in resetting the qubit by employing higher dimensional ancillas. The illustrated conditions can easily be realized by utilizing higher excited levels of transmon qubits or superconducting resonators. Such ancillas would also provide for complete controllability [7–9], which may be required to realize the spectral reshuffling of the joint initial state that implements an optimal reset dynamics, as we discuss in more detail in Appendix B.

It should be noted, however, that for an initial thermal population distribution on the ancilla, a qubit purity of exactly one can only be reached if $\rho_B$ is initially pure. This result agrees with the findings of Ref. [37], which show that if the

system and a thermal bath are initially factorized, then cooling the system to a pure state is only possible if the bath is initially at zero temperature. Proposition 1 allows us to go one step further by showing that it is possible to get $\epsilon$ close to unit purity, even if the bath is initially in a mixed state, under certain conditions (namely, ensuring that $\delta \leqslant \epsilon/[2d_{\mathrm{B}}(d_{\mathrm{S}}-1)]$, where $\delta$ represents an upper bound for a sufficient number of ancilla eigenvalues at initial time).

Moreover, our findings are in accordance with a theorem showing that cooling the system $\epsilon$ close to a pure state is possible as long as the bath initial state is sufficiently close to a so-called subsystem pure state initialization [22]. While Ref. [22] quantifies closeness primarily via the trace distance, our derivation yields a bound on the achievable system purity as a function of the spectral properties of the initial bath state.

## IV. SUMMARY

We have shown that there exists a globally minimal time (among all Hamiltonians) to reset a qubit with maximal fidelity when making use of an ancilla and time-dependent external control fields over the qubit. For two-level ancillas, a time-optimal protocol ensures resonance between qubit and ancilla and swaps their purities. The reset fidelity is then determined by the initial ancilla purity, making it crucial to engineer a sufficiently high ancilla purity or, respectively, low ancilla temperature. Due to its nontrivial dependence on the effective qubit-ancilla coupling strength, there exists an optimal choice for qubit-ancilla interaction and type of local control for the time-optimal reset. Thanks to the Cartan decomposition of SU(4), this choice can be determined at the level of the algebra, i.e., the Hamiltonian, and does not require knowledge of the actual reset dynamics. For ancillas with Hilbert space dimension larger than three, the qubit purity can be brought arbitrarily close to one by proper spectral reshuffling of the joint qubit ancilla state, provided at least half of the ancilla levels have negligible population. The corresponding experimental conditions on ancilla state and control are easily met by, e.g., current superconducting qubit technology. Our results provide the guiding principles for device design to realize the fastest and most accurate protocol for qubit reset in a given QI architecture.

## ACKNOWLEDGMENTS

We would like to thank Hoi Kwan Lau, Aashish Clerk, and Francesco Ticozzi for helpful discussions. Financial support from the Volkswagenstiftung Project No. 91004 and the ANR-DFG research program COQS (ANR-15-CE30-0023-01, DFG COQS Ko 2301/11-1) is gratefully acknowledged.

## APPENDIX A: TWO-LEVEL ANCILLAS

In the following, we provide the details of our calculations for two-level ancillas in Sec. II. In particular, in Table II, we present a detailed overview over the dynamical Lie algebras for the 27 possible choices of qubit-ancilla interaction and local control in Hamiltonian Eq. (6). In Appendix A 1, we use the time-optimal tori theorem of Ref. [12] to deduce the quantum speed limit time for qubit reset. We present details of the derivation of Eq. (8) in Appendix A 2 and discuss an extension of our model to superpositions of Pauli operators in the interaction and control Hamiltonians in Appendix A 3.

### 1. Quantum speed limit

We construct the globally minimal time to reset a qubit using a two-level ancilla, starting from a fully controllable two-qubit system and employing the time-optimal tori theorem [12]. Assuming local control over both qubit and ancilla allows us to derive the minimal time from the time-optimal tori theorem. Since our model in the main text does not include control over the ancilla, the minimum time derived here from the time-optimal tori theorem will be a lower bound for qubit reset. We show that when relaxing the controllability assumption to local control over the system qubit only, the bound is tight and can be attained for specific choices of the qubit-ancilla Hamiltonian.

For the sake of completeness, we first recall Theorems 2 and 10 of Ref. [12] in the notation of our study. We consider a system qubit coupled to a bath qubit (ancilla), described by the Hamiltonian

$$\mathsf{H} = \mathsf{H}_{\mathrm{S}} \otimes \mathbb{1}_{\mathrm{B}} + \mathbb{1}_{\mathrm{S}} \otimes \mathsf{H}_{\mathrm{B}} + \mathsf{H}_{\mathrm{int}}, \tag{A1}$$

with

$$\begin{aligned} \mathsf{H}_{\mathrm{S}} &= u_{1,\mathrm{S}}\,\sigma_1 + u_{2,\mathrm{S}}\,\sigma_2 + u_{3,\mathrm{S}}\,\sigma_3, \\ \mathsf{H}_{\mathrm{B}} &= u_{1,\mathrm{B}}\,\sigma_1 + u_{2,\mathrm{B}}\,\sigma_2 + u_{3,\mathrm{B}}\,\sigma_3, \\ \mathsf{H}_{\mathrm{int}} &= J\,\sigma_k \otimes \sigma_l, \end{aligned}$$

where $\sigma_k$, $\sigma_l \in \{\sigma_1, \sigma_2, \sigma_3\}$, and $J$ is a constant coupling strength. In contrast to our study, Ref. [12] assumes complete controllability, i.e., local controls on qubit and ancilla generating the subgroup $K = \mathrm{SU}(2) \otimes \mathrm{SU}(2)$. The dynamical Lie algebra corresponding to Eq. (A1) is thus $\mathfrak{su}(4)$. No limitations on the maximum intensity of the control fields $u_{i,\mathrm{S}}$ and $u_{i,\mathrm{B}}$ are imposed so any local operation can be realized in arbitrarily short time, which can be neglected compared to the timescale of the interaction $1/J$.

*Theorem 1 (time-optimal tori theorem* [12]). For the system described by Eq. (A1), the minimum time to generate a unitary propagator $\mathsf{U}_{\mathrm{F}} \in \mathrm{SU}(4)$ corresponds to the smallest value of $\sum_k c_k$, where $c_k \in [0, \pi]$, such that

$$\mathsf{U}_{\mathrm{F}} = \mathsf{K} e^{\frac{\mathrm{i}}{2}\sum_k c_k \sigma_k \otimes \sigma_k} \mathsf{K}',$$

with $\mathsf{K}, \mathsf{K}' \in K$. The minimum time $T$ is given by $T = \frac{1}{2J}\sum_k c_k$.

The proof of Theorem 1 [12] is based on the same Cartan decomposition of SU(4) as used in the main text. A minimum-time control strategy can be derived from Theorem 1 by expressing the propagator $\mathsf{U}_{\mathrm{F}}$ as

$$\begin{aligned} \mathsf{U}_{\mathrm{F}} &= \mathsf{K}\left(\prod_{k=1}^{3} e^{\frac{\mathrm{i}}{2} c_k \sigma_k \otimes \sigma_k}\right)\mathsf{K}' \\ &= \mathsf{K}_1' e^{\frac{\mathrm{i}}{2J} c_1 \mathsf{H}_{\mathrm{int}}} \mathsf{K}_2' e^{\frac{\mathrm{i}}{2J} c_2 \mathsf{H}_{\mathrm{int}}} \mathsf{K}_3' e^{\frac{\mathrm{i}}{2J} c_3 \mathsf{H}_{\mathrm{int}}} \mathsf{K}_4', \end{aligned}$$

where $\mathsf{K}_1', \mathsf{K}_2', \mathsf{K}_3', \mathsf{K}_4' \in K$ are chosen such that they rotate $\mathsf{H}_{\mathrm{int}}$ into the corresponding term of $\sigma_k \otimes \sigma_k$. The control protocol thus consists in a series of local pulses (which take no

TABLE II. Dynamical Lie algebras $\mathcal{L}$, their respective Cartan decompositions $\mathcal{L} = \mathfrak{k} \oplus \mathfrak{p}$ and a possible choice for the Cartan subalgebra $\mathfrak{a} \subset \mathfrak{p}$ for all possible variants of Hamiltonian (6). The interaction part and the qubit control are given by $\mathsf{H}_{\text{int}} = J(\mathsf{O}_\text{S} \otimes \mathsf{O}_\text{B})$ and $\mathsf{H}_\text{c}(t) = \mathcal{E}(t)\mathsf{O}_\text{c}$, respectively.

| $\mathsf{O}_\text{S} \otimes \mathsf{O}_\text{B}$ | $\mathsf{O}_\text{c}$ | $\mathfrak{k}$ | $\mathfrak{p}$ | $\mathfrak{a}$ |
|---|---|---|---|---|
| $\sigma_1 \otimes \sigma_1$ | $\sigma_1$ | $\mathbb{1} \otimes \sigma_3, \sigma_1 \otimes \mathbb{1}, \sigma_2 \otimes \mathbb{1}, \sigma_3 \otimes \mathbb{1}$ | $\sigma_1 \otimes \sigma_1, \sigma_1 \otimes \sigma_2, \sigma_2 \otimes \sigma_1, \sigma_2 \otimes \sigma_2, \sigma_3 \otimes \sigma_1, \sigma_3 \otimes \sigma_2$ | $\sigma_1 \otimes \sigma_1, \sigma_2 \otimes \sigma_2$ |
| $\sigma_1 \otimes \sigma_1$ | $\sigma_2$ | $\mathbb{1} \otimes \sigma_3, \sigma_1 \otimes \mathbb{1}, \sigma_2 \otimes \mathbb{1}, \sigma_3 \otimes \mathbb{1}$ | $\sigma_1 \otimes \sigma_1, \sigma_1 \otimes \sigma_2, \sigma_2 \otimes \sigma_1, \sigma_2 \otimes \sigma_2, \sigma_3 \otimes \sigma_1, \sigma_3 \otimes \sigma_2$ | $\sigma_1 \otimes \sigma_1, \sigma_2 \otimes \sigma_2$ |
| $\sigma_1 \otimes \sigma_1$ | $\sigma_3$ | $\mathbb{1} \otimes \sigma_3, \sigma_3 \otimes \mathbb{1}$ | $\sigma_1 \otimes \sigma_1, \sigma_1 \otimes \sigma_2, \sigma_2 \otimes \sigma_1, \sigma_2 \otimes \sigma_2$ | $\sigma_1 \otimes \sigma_1, \sigma_2 \otimes \sigma_2$ |
| $\sigma_1 \otimes \sigma_2$ | $\sigma_1$ | $\mathbb{1} \otimes \sigma_3, \sigma_1 \otimes \mathbb{1}, \sigma_2 \otimes \mathbb{1}, \sigma_3 \otimes \mathbb{1}$ | $\sigma_1 \otimes \sigma_1, \sigma_1 \otimes \sigma_2, \sigma_2 \otimes \sigma_1, \sigma_2 \otimes \sigma_2, \sigma_3 \otimes \sigma_1, \sigma_3 \otimes \sigma_2$ | $\sigma_1 \otimes \sigma_1, \sigma_2 \otimes \sigma_2$ |
| $\sigma_1 \otimes \sigma_2$ | $\sigma_2$ | $\mathbb{1} \otimes \sigma_3, \sigma_1 \otimes \mathbb{1}, \sigma_2 \otimes \mathbb{1}, \sigma_3 \otimes \mathbb{1}$ | $\sigma_1 \otimes \sigma_1, \sigma_1 \otimes \sigma_2, \sigma_2 \otimes \sigma_1, \sigma_2 \otimes \sigma_2, \sigma_3 \otimes \sigma_1, \sigma_3 \otimes \sigma_2$ | $\sigma_1 \otimes \sigma_1, \sigma_2 \otimes \sigma_2$ |
| $\sigma_1 \otimes \sigma_2$ | $\sigma_3$ | $\mathbb{1} \otimes \sigma_3, \sigma_3 \otimes \mathbb{1}$ | $\sigma_1 \otimes \sigma_1, \sigma_1 \otimes \sigma_2, \sigma_2 \otimes \sigma_1, \sigma_2 \otimes \sigma_2$ | $\sigma_1 \otimes \sigma_1, \sigma_2 \otimes \sigma_2$ |
| $\sigma_1 \otimes \sigma_3$ | $\sigma_1$ | $\mathbb{1} \otimes \sigma_3, \sigma_1 \otimes \mathbb{1}, \sigma_2 \otimes \mathbb{1}, \sigma_3 \otimes \mathbb{1}$ | $\sigma_1 \otimes \sigma_3, \sigma_2 \otimes \sigma_3, \sigma_3 \otimes \sigma_3$ | $\sigma_3 \otimes \sigma_3$ |
| $\sigma_1 \otimes \sigma_3$ | $\sigma_2$ | $\mathbb{1} \otimes \sigma_3, \sigma_1 \otimes \mathbb{1}, \sigma_2 \otimes \mathbb{1}, \sigma_3 \otimes \mathbb{1}$ | $\sigma_1 \otimes \sigma_3, \sigma_2 \otimes \sigma_3, \sigma_3 \otimes \sigma_3$ | $\sigma_3 \otimes \sigma_3$ |
| $\sigma_1 \otimes \sigma_3$ | $\sigma_3$ | $\mathbb{1} \otimes \sigma_3, \sigma_3 \otimes \mathbb{1}$ | $\sigma_1 \otimes \sigma_3, \sigma_2 \otimes \sigma_3$ | $\sigma_1 \otimes \sigma_3$ |
| $\sigma_2 \otimes \sigma_1$ | $\sigma_1$ | $\mathbb{1} \otimes \sigma_3, \sigma_1 \otimes \mathbb{1}, \sigma_2 \otimes \mathbb{1}, \sigma_3 \otimes \mathbb{1}$ | $\sigma_1 \otimes \sigma_1, \sigma_1 \otimes \sigma_2, \sigma_2 \otimes \sigma_1, \sigma_2 \otimes \sigma_2, \sigma_3 \otimes \sigma_1, \sigma_3 \otimes \sigma_2$ | $\sigma_1 \otimes \sigma_1, \sigma_2 \otimes \sigma_2$ |
| $\sigma_2 \otimes \sigma_1$ | $\sigma_2$ | $\mathbb{1} \otimes \sigma_3, \sigma_1 \otimes \mathbb{1}, \sigma_2 \otimes \mathbb{1}, \sigma_3 \otimes \mathbb{1}$ | $\sigma_1 \otimes \sigma_1, \sigma_1 \otimes \sigma_2, \sigma_2 \otimes \sigma_1, \sigma_2 \otimes \sigma_2, \sigma_3 \otimes \sigma_1, \sigma_3 \otimes \sigma_2$ | $\sigma_1 \otimes \sigma_1, \sigma_2 \otimes \sigma_2$ |
| $\sigma_2 \otimes \sigma_1$ | $\sigma_3$ | $\mathbb{1} \otimes \sigma_3, \sigma_3 \otimes \mathbb{1}$ | $\sigma_1 \otimes \sigma_1, \sigma_1 \otimes \sigma_2, \sigma_2 \otimes \sigma_1, \sigma_2 \otimes \sigma_2$ | $\sigma_1 \otimes \sigma_1, \sigma_2 \otimes \sigma_2$ |
| $\sigma_2 \otimes \sigma_2$ | $\sigma_1$ | $\mathbb{1} \otimes \sigma_3, \sigma_1 \otimes \mathbb{1}, \sigma_2 \otimes \mathbb{1}, \sigma_3 \otimes \mathbb{1}$ | $\sigma_1 \otimes \sigma_1, \sigma_1 \otimes \sigma_2, \sigma_2 \otimes \sigma_1, \sigma_2 \otimes \sigma_2, \sigma_3 \otimes \sigma_1, \sigma_3 \otimes \sigma_2$ | $\sigma_1 \otimes \sigma_1, \sigma_2 \otimes \sigma_2$ |
| $\sigma_2 \otimes \sigma_2$ | $\sigma_2$ | $\mathbb{1} \otimes \sigma_3, \sigma_1 \otimes \mathbb{1}, \sigma_2 \otimes \mathbb{1}, \sigma_3 \otimes \mathbb{1}$ | $\sigma_1 \otimes \sigma_1, \sigma_1 \otimes \sigma_2, \sigma_2 \otimes \sigma_1, \sigma_2 \otimes \sigma_2, \sigma_3 \otimes \sigma_1, \sigma_3 \otimes \sigma_2$ | $\sigma_1 \otimes \sigma_1, \sigma_2 \otimes \sigma_2$ |
| $\sigma_2 \otimes \sigma_2$ | $\sigma_3$ | $\mathbb{1} \otimes \sigma_3, \sigma_3 \otimes \mathbb{1}$ | $\sigma_1 \otimes \sigma_1, \sigma_1 \otimes \sigma_2, \sigma_2 \otimes \sigma_1, \sigma_2 \otimes \sigma_2$ | $\sigma_1 \otimes \sigma_1, \sigma_2 \otimes \sigma_2$ |
| $\sigma_2 \otimes \sigma_3$ | $\sigma_1$ | $\mathbb{1} \otimes \sigma_3, \sigma_1 \otimes \mathbb{1}, \sigma_2 \otimes \mathbb{1}, \sigma_3 \otimes \mathbb{1}$ | $\sigma_1 \otimes \sigma_3, \sigma_2 \otimes \sigma_3, \sigma_3 \otimes \sigma_3$ | $\sigma_3 \otimes \sigma_3$ |
| $\sigma_2 \otimes \sigma_3$ | $\sigma_2$ | $\mathbb{1} \otimes \sigma_3, \sigma_1 \otimes \mathbb{1}, \sigma_2 \otimes \mathbb{1}, \sigma_3 \otimes \mathbb{1}$ | $\sigma_1 \otimes \sigma_3, \sigma_2 \otimes \sigma_3, \sigma_3 \otimes \sigma_3$ | $\sigma_3 \otimes \sigma_3$ |
| $\sigma_2 \otimes \sigma_3$ | $\sigma_3$ | $\mathbb{1} \otimes \sigma_3, \sigma_3 \otimes \mathbb{1}$ | $\sigma_1 \otimes \sigma_3, \sigma_2 \otimes \sigma_3$ | $\sigma_1 \otimes \sigma_3$ |
| $\sigma_3 \otimes \sigma_1$ | $\sigma_1$ | $\mathbb{1} \otimes \sigma_3, \sigma_1 \otimes \mathbb{1}, \sigma_2 \otimes \mathbb{1}, \sigma_3 \otimes \mathbb{1}$ | $\sigma_1 \otimes \sigma_1, \sigma_1 \otimes \sigma_2, \sigma_2 \otimes \sigma_1, \sigma_2 \otimes \sigma_2, \sigma_3 \otimes \sigma_1, \sigma_3 \otimes \sigma_2$ | $\sigma_1 \otimes \sigma_1, \sigma_2 \otimes \sigma_2$ |
| $\sigma_3 \otimes \sigma_1$ | $\sigma_2$ | $\mathbb{1} \otimes \sigma_3, \sigma_1 \otimes \mathbb{1}, \sigma_2 \otimes \mathbb{1}, \sigma_3 \otimes \mathbb{1}$ | $\sigma_1 \otimes \sigma_1, \sigma_1 \otimes \sigma_2, \sigma_2 \otimes \sigma_1, \sigma_2 \otimes \sigma_2, \sigma_3 \otimes \sigma_1, \sigma_3 \otimes \sigma_2$ | $\sigma_1 \otimes \sigma_1, \sigma_2 \otimes \sigma_2$ |
| $\sigma_3 \otimes \sigma_1$ | $\sigma_3$ | $\mathbb{1} \otimes \sigma_3, \sigma_3 \otimes \mathbb{1}$ | $\sigma_3 \otimes \sigma_1, \sigma_3 \otimes \sigma_2$ | $\sigma_3 \otimes \sigma_1$ |
| $\sigma_3 \otimes \sigma_2$ | $\sigma_1$ | $\mathbb{1} \otimes \sigma_3, \sigma_1 \otimes \mathbb{1}, \sigma_2 \otimes \mathbb{1}, \sigma_3 \otimes \mathbb{1}$ | $\sigma_1 \otimes \sigma_1, \sigma_1 \otimes \sigma_2, \sigma_2 \otimes \sigma_1, \sigma_2 \otimes \sigma_2, \sigma_3 \otimes \sigma_1, \sigma_3 \otimes \sigma_2$ | $\sigma_1 \otimes \sigma_1, \sigma_2 \otimes \sigma_2$ |
| $\sigma_3 \otimes \sigma_2$ | $\sigma_2$ | $\mathbb{1} \otimes \sigma_3, \sigma_1 \otimes \mathbb{1}, \sigma_2 \otimes \mathbb{1}, \sigma_3 \otimes \mathbb{1}$ | $\sigma_1 \otimes \sigma_1, \sigma_1 \otimes \sigma_2, \sigma_2 \otimes \sigma_1, \sigma_2 \otimes \sigma_2, \sigma_3 \otimes \sigma_1, \sigma_3 \otimes \sigma_2$ | $\sigma_1 \otimes \sigma_1, \sigma_2 \otimes \sigma_2$ |
| $\sigma_3 \otimes \sigma_2$ | $\sigma_3$ | $\mathbb{1} \otimes \sigma_3, \sigma_3 \otimes \mathbb{1}$ | $\sigma_3 \otimes \sigma_1, \sigma_3 \otimes \sigma_2$ | $\sigma_3 \otimes \sigma_1$ |
| $\sigma_3 \otimes \sigma_3$ | $\sigma_1$ | $\mathbb{1} \otimes \sigma_3, \sigma_1 \otimes \mathbb{1}, \sigma_2 \otimes \mathbb{1}, \sigma_3 \otimes \mathbb{1}$ | $\sigma_1 \otimes \sigma_3, \sigma_2 \otimes \sigma_3, \sigma_3 \otimes \sigma_3$ | $\sigma_3 \otimes \sigma_3$ |
| $\sigma_3 \otimes \sigma_3$ | $\sigma_2$ | $\mathbb{1} \otimes \sigma_3, \sigma_1 \otimes \mathbb{1}, \sigma_2 \otimes \mathbb{1}, \sigma_3 \otimes \mathbb{1}$ | $\sigma_1 \otimes \sigma_3, \sigma_2 \otimes \sigma_3, \sigma_3 \otimes \sigma_3$ | $\sigma_3 \otimes \sigma_3$ |
| $\sigma_3 \otimes \sigma_3$ | $\sigma_3$ | $\mathbb{1} \otimes \sigma_3, \sigma_3 \otimes \mathbb{1}$ | $\sigma_3 \otimes \sigma_3$ | $\sigma_3 \otimes \sigma_3$ |

time) and field-free evolutions under the interaction Hamiltonian $\mathsf{H}_{\text{int}}$ [of duration $c_k/(2J)$]. We now apply Theorem 1 to qubit reset, taking the initial state as $\rho(0) = \mathbb{1}/2 \otimes \rho_\text{B}(0)$ with $\mathcal{P}_\text{B}(0) = \text{tr}\{\rho_\text{B}^2(0)\}$ the initial ancilla purity. To simplify the description, we assume the qubit to be initially in the maximally mixed state, which is the state requiring the largest entropy or purity change. The initial ancilla state is written as

$$\rho_\text{B}(0) = \begin{pmatrix} p_\text{B}^\text{e} & \gamma_\text{B} \\ \gamma_\text{B}^* & p_\text{B}^\text{g} \end{pmatrix},$$

with $\mathcal{P}_\text{B}(0) = (p_\text{B}^\text{g})^2 + (p_\text{B}^\text{e})^2 + 2|\gamma_\text{B}|^2$. Denoting the evolution operator that realizes the qubit reset in minimum time, $T_{\text{min}}$, by $\mathsf{U}_\text{F}$ and using Theorem 1, we obtain

$$\rho_\text{S}(T_{\text{min}}) = \text{tr}_\text{B}\{\mathsf{U}_\text{F}\rho(0)\mathsf{U}_\text{F}^\dagger\}.$$

Inserting $\mathsf{U}_\text{F}$ from Theorem 1 leads to

$$\begin{aligned}\rho_\text{S}(T_{\text{min}}) = \mathbb{1}/2 &+ \mathfrak{Re}(\gamma_\text{B}')\sin(c_2)\sin(c_3)\,\sigma_1 \\ &- \mathfrak{Im}(\gamma_\text{B}')\sin(c_1)\sin(c_3)\,\sigma_2 \\ &- \tfrac{1}{2}\left(p_\text{B}^{\text{g}'} - p_\text{B}^{\text{e}'}\right)\sin(c_1)\sin(c_2)\,\sigma_3,\end{aligned}$$

where $p_\text{B}^{\text{g}'}$, $p_\text{B}^{\text{e}'}$, and $\gamma_\text{B}'$ are the matrix elements of $\rho_\text{B}(0)$ in a new basis,

$$\begin{pmatrix} p_\text{B}^{\text{e}'} & \gamma_\text{B}' \\ \gamma_\text{B}'^* & p_\text{B}^{\text{g}'} \end{pmatrix} = \mathsf{k}_\text{B}\begin{pmatrix} p_\text{B}^\text{e} & \gamma_\text{B} \\ \gamma_\text{B}^* & p_\text{B}^\text{g} \end{pmatrix}\mathsf{k}_\text{B}^\dagger$$

with $\mathsf{k}_\text{B}$ being a unitary local operation on the ancilla. The coefficients $p_\text{B}^{\text{g}'}$, $p_\text{B}^{\text{e}'}$ and $\gamma_\text{B}'$ fulfill the constraint

$$\mathcal{P}_\text{B}(0) = \left(p_\text{B}^{\text{g}'}\right)^2 + \left(p_\text{B}^{\text{e}'}\right)^2 + 2|\gamma_\text{B}'|^2, \tag{A2}$$

since local operations cannot change the ancilla purity. The qubit purity at time $T_{\text{min}}$ becomes

$$\begin{aligned}\mathcal{P}_\text{S}(T_{\text{min}}) &= \text{tr}\left\{\rho_\text{S}^2(T_{\text{min}})\right\} \\ &= \tfrac{1}{2} + \left(\left(p_\text{B}^{\text{g}'}\right)^2 + \left(p_\text{B}^{\text{e}'}\right)^2 - \tfrac{1}{2}\right)\sin^2(c_1)\sin^2(c_2) \\ &\quad + 2\,\mathfrak{Re}(\gamma_\text{B}')^2\sin^2(c_2)\sin^2(c_3) \\ &\quad + 2\,\mathfrak{Im}(\gamma_\text{B}')^2\sin^2(c_1)\sin^2(c_3)\end{aligned} \tag{A3}$$

and is upper bounded by

$$\begin{aligned}\mathcal{P}_\text{S}(T_{\text{min}}) &\leqslant \left(p_\text{B}^{\text{g}'}\right)^2 + \left(p_\text{B}^{\text{e}'}\right)^2 + 2\,\mathfrak{Re}(\gamma_\text{B}')^2 + 2\,\mathfrak{Im}(\gamma_\text{B}')^2 \\ &= \mathcal{P}_\text{B}(0),\end{aligned}$$

i.e., the maximum qubit purity $\mathcal{P}_S(T_{\min})$ is the initial purity $\mathcal{P}_B(0)$ of the ancilla [22].

This upper bound can be attained, for instance, if $c_1 = c_2 = c_3 = \frac{\pi}{2}$. Employing Theorem 1, this leads to a control time $T = \frac{3\pi}{4J}$. Note that this control strategy works for any value of $p_B^{g'}$, $p_B^{e'}$, and $\gamma_B'$. However, this time is not the minimum time and shorter durations can be found under certain assumptions on $p_B^{g'}$, $p_B^{e'}$, and $\gamma_B'$, or rather on the local transformation $\mathsf{k}_B$, as we show next.

Direct analysis of Eq. (A3) reveals that the maximum purity can be attained in time $T = \pi/(2J)$ for three symmetric processes in which one of the three parameters $c_k$ is zero and the other two equal $\pi/2$. Whether it is possible to utilize one of these strategies depends on the local transformation $\mathsf{k}_B$ of the ancilla. If, for example, $\gamma_B' = 0$ and hence $\mathcal{P}_B(0) = (p_B^{g'})^2 + (p_B^{e'})^2$, setting $c_3 = 0$ yields a purification time $T = \pi/(2J)$. These requirements are fulfilled if the ancilla is initially in thermal equilibrium and the local transformation $\mathsf{k}_B$ is generated only by $\sigma_3$. Similarly, we find for $\mathfrak{Re}(\gamma_B')^2 = \frac{\mathcal{P}_B(0)}{2} - \frac{1}{4}$ that $c_1 = 0$ allows for fast purification and with $c_2 = 0$ this time can be achieved if $\mathfrak{Im}(\gamma_B')^2 = \frac{\mathcal{P}_B(0)}{2} - \frac{1}{4}$. We prove in Theorem 2 that these protocols are the time-optimal strategies for qubit reset with the Hamiltonian Eq. (A1).

*Theorem 2.* Given Eq. (A1), the minimum time to reset the qubit and reach the maximum possible purity from a maximally mixed state is $T_{\min} = \pi/(2J)$. The time-optimal control strategies correspond to the cases where two of the $c_k$ in $\mathsf{U}_F$ are equal to $\pi/2$ and the third one is zero. The control protocol depends on the local operation on the ancilla characterized by the parameters $p_B^{g'}$, $p_B^{e'}$, and $\gamma_B'$ and is optimized to attain maximum purity.

*Proof.* Using Eq. (A2), we find for the qubit purity

$$\begin{aligned}\mathcal{P}_S(T_{\min}) = {} & \tfrac{1}{2} + \left(\mathcal{P}_B(0) - \tfrac{1}{2}\right)\sin^2(c_1)\sin^2(c_2) \\ & + 2\mathfrak{Re}(\gamma_B')^2\sin^2(c_2)[\sin^2(c_3) - \sin^2(c_1)] \\ & + 2\mathfrak{Im}(\gamma_B')^2\sin^2(c_1)[\sin^2(c_3) - \sin^2(c_2)], \quad \text{(A4)}\end{aligned}$$

i.e., the qubit purity can be interpreted as a function $F_{\gamma_B'}$ of $(c_1, c_2, c_3) \in [0, \pi]^3$ parameterized by $\gamma_B'$. A maximum of $F_{\gamma_B'}$ fulfills the necessary conditions $\partial_{c_1} F_{\gamma_B'} = \partial_{c_2} F_{\gamma_B'} = \partial_{c_3} F_{\gamma_B'} = 0$, where $\partial_{c_k}$ denotes the partial derivative with respect to $c_k$. We obtain the following system of equations:

$$\sin(2c_1)\left[\left(\frac{\mathcal{P}_B(0)}{2} - \frac{1}{4} - \mathfrak{Re}(\gamma_B')^2 - \mathfrak{Im}(\gamma_B')^2\right)\sin^2(c_2) + \mathfrak{Im}(\gamma_B')^2\sin^2(c_3)\right] = 0, \quad \text{(A5a)}$$

$$\sin(2c_2)\left[\left(\frac{\mathcal{P}_B(0)}{2} - \frac{1}{4} - \mathfrak{Re}(\gamma_B')^2 - \mathfrak{Im}(\gamma_B')^2\right)\sin^2(c_1) + \mathfrak{Re}(\gamma_B')^2\sin^2(c_3)\right] = 0, \quad \text{(A5b)}$$

$$\sin(2c_3)\left[\mathfrak{Re}(\gamma_B')^2\sin^2(c_2) + \mathfrak{Im}(\gamma_B')^2\sin^2(c_1)\right] = 0. \quad \text{(A5c)}$$

We study below the different extrema of $F_{\gamma_B'}$ that allow us to achieve maximum purity in a time shorter or equal to $\pi/(2J)$, i.e., for $c_1 + c_2 + c_3 \leqslant \pi$. We do not consider the other cases.

First, we examine Eq. (A5c) and realize that it is satisfied if $\sin(2c_3) = 0$, leading to $c_3 = 0$ or $c_3 = \pi/2$ (the case $c_3 = \pi$ is not relevant). In the former case, we can deduce from Eqs. (A4) and (A5) that $c_1 = c_2 = \pi/2$ is a solution under the requirement $\mathfrak{Re}(\gamma_B') = \mathfrak{Im}(\gamma_B') = 0$. This is, as before, a condition on the local operation $\mathsf{k}_B$. The other choice, $c_3 = \pi/2$, yields two possible solutions for $c_1$ and $c_2$, which again are constrained by the local transformation $\mathsf{k}_B$. If $\mathfrak{Im}(\gamma_B')^2 = \frac{\mathcal{P}_B(0)}{2} - \frac{1}{4}$, the equations are solved with $c_1 = \pi/2$ and $c_2 = 0$, while for $\mathfrak{Re}(\gamma_B')^2 = \frac{\mathcal{P}_B(0)}{2} - \frac{1}{4}$, the solution reads $c_1 = 0$ and $c_2 = \pi/2$. This leaves us with three possible control strategies, but all of them obey $c_1 + c_2 + c_3 = \pi$ and therefore lead to a reset time of $T_{\min} = \pi/(2J)$. Finally, we also have to consider $\mathfrak{Re}(\gamma_B')^2\sin^2(c_2) + \mathfrak{Im}(\gamma_B')^2\sin^2(c_1) = 0$, which is, in addition to $\sin(2c_3) = 0$, the second solution to Eq. (A5c). The only relevant case corresponds to $\mathfrak{Re}(\gamma_B') = \mathfrak{Im}(\gamma_B') = 0$, which leads to $c_1 = c_2 = \pi/2$ and we retrieve one of the previous solutions. The same analysis can be carried out for the other two equations, leading to the same solutions. This indeed shows that considering all possibilities, it is not possible to solve Eqs. (A5) with $c_1 + c_2 + c_3 < \pi$ and therefore completes the proof. ∎

Theorem 2 tells us that the shortest possible time $T_{\min}$ to reset the qubit is

$$T_{\min} = \frac{\pi}{2J}.$$

We show in the main text that this lower bound can be attained for several choices of control and interaction Hamiltonians, highlighting the tightness of the bound. Attaining the bound for qubit reset is possible without the need for local control over the ancilla, i.e., without complete controllability. Note that the control procedure derived in the main text, i.e., the resonant protocol, is completely different from the time-optimal strategy predicted by Theorem 1, consisting in a concatenation of local hard pulses and free evolutions [12].

Most importantly, our results imply that local control over the qubit ancilla does not allow us to improve the reset time.

### 2. Maximum purity and minimum reset time for qubit and ancilla on resonance

We explain now how to obtain the closed-form expression for the time evolution of the qubit purity, Eq. (8) of the main text, given that the joint qubit-ancilla dynamics is described by Hamiltonian Eq. (6). We present a detailed derivation for $\mathsf{H}_{\text{int}} = J(\sigma_1 \otimes \sigma_1)$ and $\mathsf{H}_c = \mathcal{E}\sigma_1$, i.e., $\mathsf{O}_S = \mathsf{O}_B = \mathsf{O}_c = \sigma_1$ and explain how to extend the derivation to all other possible combinations of $\mathsf{O}_S, \mathsf{O}_B, \mathsf{O}_c \in \{\sigma_1, \sigma_2, \sigma_3\}$ which fulfill

$\dim\{\mathfrak{a}\} = 2$, cf. Table II, presenting all possible realizations for Hamiltonian Eq. (6).

We start by applying a transformation $\mathsf{T} = \mathsf{T}_\mathrm{S} \otimes \mathbb{1}_\mathrm{B}$, where $\mathsf{T}_\mathrm{S}$ is chosen such that it diagonalizes $\mathsf{H}_\mathrm{S}$. The transformed Hamiltonian $\mathsf{H}' = \mathsf{T}^\dagger \mathsf{H} \mathsf{T}$ for a constant and resonant field $\mathcal{E}$ becomes

$$\mathsf{H}' = \begin{pmatrix} \omega_\mathrm{B} & B & 0 & A \\ B & 0 & A & 0 \\ 0 & A & 0 & -B \\ A & 0 & -B & -\omega_\mathrm{B} \end{pmatrix}, \tag{A6}$$

with $A = J\omega_\mathrm{S}/\omega_\mathrm{B}$ and $B = 2J\mathcal{E}/\omega_\mathrm{B}$. The resonance condition for this choice of Hamiltonian implies $\mathcal{E}(t) = \mathcal{E} = \sqrt{\omega_\mathrm{B}^2 - \omega_\mathrm{S}^2}/2$ and, as a consequence, $|A|^2 + |B|^2 = J^2$. For the constant resonant field, the time-evolution operator $\mathsf{U}(t)$ can be calculated analytically,

$$\mathsf{U}(t) = e^{-\mathrm{i}\mathsf{H}'t} = \begin{pmatrix} u_{11} & u_{12} & u_{13} & u_{14} \\ u_{12} & u_{22} & u_{23} & u_{13} \\ u_{13} & u_{23} & u_{22}^* & u_{12}^* \\ u_{14} & u_{13} & u_{12}^* & u_{11}^* \end{pmatrix}, \tag{A7}$$

with

$$\begin{aligned} u_{11} &= \frac{\delta_+}{2}\cos(\Phi_+) + \frac{\delta_-}{2}\cos(\Phi_-) \\ &\quad - \mathrm{i}\frac{1}{\eta_+}\left(\frac{\delta_+\omega_\mathrm{B}}{2} + \frac{|B|^2}{\Omega}\right)\sin(\Phi_+) \\ &\quad - \mathrm{i}\frac{1}{\eta_-}\left(\frac{\delta_-\omega_\mathrm{B}}{2} - \frac{|B|^2}{\Omega}\right)\sin(\Phi_-), \end{aligned} \tag{A8a}$$

$$\begin{aligned} u_{12} &= \frac{B}{\Omega}(\cos(\Phi_+) - \cos(\Phi_-)) \\ &\quad - \mathrm{i}\frac{B}{2}\left(\frac{\delta_+}{\eta_+}\sin(\Phi_+) + \frac{\delta_-}{\eta_-}\sin(\Phi_-)\right), \end{aligned} \tag{A8b}$$

$$u_{13} = -\mathrm{i}\frac{AB}{\Omega}\left(\frac{1}{\eta_+}\sin(\Phi_+) - \frac{1}{\eta_-}\sin(\Phi_-)\right), \tag{A8c}$$

$$u_{14} = -\mathrm{i}\frac{A}{2}\left(\frac{\delta_+}{\eta_+}\sin(\Phi_+) + \frac{\delta_-}{\eta_-}\sin(\Phi_-)\right), \tag{A8d}$$

$$\begin{aligned} u_{22} &= \frac{\delta_+}{2}\cos(\Phi_-) + \frac{\delta_-}{2}\cos(\Phi_+) \\ &\quad - \mathrm{i}\frac{|B|^2}{\eta_+\Omega}\sin(\Phi_+) + \mathrm{i}\frac{|B|^2}{\eta_-\Omega}\sin(\Phi_-), \end{aligned} \tag{A8e}$$

$$u_{23} = -\mathrm{i}\frac{A}{2}\left(\frac{\delta_+}{\eta_-}\sin(\Phi_-) + \frac{\delta_-}{\eta_+}\sin(\Phi_+)\right), \tag{A8f}$$

where $\delta_\pm = 1 \pm \omega_\mathrm{B}/\Omega$, $\Omega = \sqrt{\omega_\mathrm{B}^2 + 4|B|^2}$,

$$\eta_\pm = \sqrt{J^2 + \frac{\omega_\mathrm{B}}{2}(\omega_\mathrm{B} \pm \Omega)} \tag{A9}$$

and $\Phi_\pm(t) = \eta_\pm t$. Note that $\Phi_\pm(t)$ is the only time-dependent quantity in Eqs. (A8).

We can approximate Eqs. (A7) and (A8), which are exact, to derive an expression for the qubit purity:

$$\mathcal{P}_\mathrm{S}(t) = \mathrm{tr}\left\{\mathrm{tr}_\mathrm{B}^2\{\mathsf{U}(t)\rho(0)\mathsf{U}^\dagger(t)\}\right\}. \tag{A10}$$

Each element of the time-evolution operator is given by a sum of trigonometric functions. We thus compare their amplitudes to identify the dominating terms. As an illustration, the approximations will be explicitly shown for the amplitude of the final term of $u_{11}$ in Eq. (A8a), but the procedure is equivalent for all other contributions. Using the relation $J = \sqrt{|A|^2 + |B|^2}$, we express all variables in terms of $A$, $B$, and $\omega_\mathrm{B}$. For the final term in Eq. (A8a), this results in

$$\delta_- = 1 - \frac{\omega_\mathrm{B}}{2\sqrt{\omega_\mathrm{B}^2 + |B|^2}} \tag{A11a}$$

and

$$\eta_- = \sqrt{|A|^2 + |B|^2 + \frac{\omega_\mathrm{B}^2}{2} - \frac{\omega_\mathrm{B}}{2}\sqrt{\omega_\mathrm{B}^2 + 4|B|^2}}. \tag{A11b}$$

Typically, $J \ll \omega_\mathrm{B}$. Since $|B| \leqslant J$, this suggests an expansion of all variables in $B$,

$$\delta_- \approx \frac{2|B|^2}{\omega_\mathrm{B}^2} + \mathcal{O}(|B|^4), \tag{A12a}$$

$$\eta_- \approx |A| + \mathcal{O}(|B|^4), \tag{A12b}$$

$$\Omega \approx \omega_\mathrm{B} + \frac{2|B|^2}{\omega_\mathrm{B}^2} + \mathcal{O}(|B|^4). \tag{A12c}$$

With the approximated variables, we find

$$\frac{\mathrm{i}}{\eta_-}\left(\delta_-\omega_\mathrm{B} - 2|B|^2/\Omega\right) \approx \mathcal{O}(|B|^4), \tag{A13}$$

i.e., we can neglect the final term in Eq. (A8a). Carrying out similar approximations for the other amplitudes in Eqs. (A8) leads to

$$u_{11} \approx \cos(\Phi_+) - \mathrm{i}\sin(\Phi_+), \tag{A14a}$$

$$u_{12} \approx 0, \tag{A14b}$$

$$u_{13} \approx 0, \tag{A14c}$$

$$u_{14} \approx 0, \tag{A14d}$$

$$u_{22} \approx \cos(\Phi_-), \tag{A14e}$$

$$u_{23} \approx \mathrm{i}\sin(\Phi_-). \tag{A14f}$$

The corresponding approximated time-evolution operator allows us to obtain a closed-form expression for the time evolution of the qubit purity $\mathcal{P}_\mathrm{S}(t)$. To derive it, we additionally assume the initial state of qubit and ancilla to be separable and the ancilla to be in thermal equilibrium with its bath, cf. Eq. (7) in the main text. The qubit purity, cf. Eq. (A10), is then given by

$$\begin{aligned} \mathcal{P}_\mathrm{S}(t) &= \left[p_\mathrm{S}^\mathrm{e}p_\mathrm{B}^\mathrm{e}|u_{11}|^2 + p_\mathrm{S}^\mathrm{e}p_\mathrm{B}^\mathrm{g}|u_{22}|^2 + p_\mathrm{S}^\mathrm{g}p_\mathrm{B}^\mathrm{e}|u_{23}|^2\right]^2 \\ &\quad + \left[p_\mathrm{S}^\mathrm{g}p_\mathrm{B}^\mathrm{g}|u_{11}|^2 + p_\mathrm{S}^\mathrm{g}p_\mathrm{B}^\mathrm{e}|u_{22}|^2 + p_\mathrm{S}^\mathrm{e}p_\mathrm{B}^\mathrm{g}|u_{23}|^2\right]^2 \\ &\quad + 2|\gamma_\mathrm{S}|^2|u_{11}|^2|u_{22}|^2. \end{aligned} \tag{A15}$$

Note that the qubit purity $\mathcal{P}_\mathrm{S}(t)$ depends only on $\eta_-$. While $u_{11}$ depends on $\eta_+$, cf. Eq. (A14), it enters $\mathcal{P}_\mathrm{S}(t)$ as $|u_{11}|^2 \approx 1$ such that the dependence on $\eta_+$ disappears when inserting Eq. (A14) and $\Phi_\pm = \eta_\pm t$ into Eq. (A15). Relabeling $\eta_-$ by $\eta$, we obtain Eq. (8) of the main text.

For all the other combinations in Table II with $\dim\{\mathfrak{a}\} = 2$, one just has to consider slightly modified forms of the Hamiltonian $\mathsf{H}'_1 = \mathsf{H}'$ in Eq. (A6), namely,

$$\mathsf{H}'_2 = \begin{pmatrix} \omega_B & B & 0 & -A \\ -B & 0 & A & 0 \\ 0 & -A & 0 & -B \\ A & 0 & B & -\omega_B \end{pmatrix}, \tag{A16a}$$

or

$$\mathsf{H}'_3 = \begin{pmatrix} \omega_B & 0 & 0 & -A \\ 0 & 0 & -A & 0 \\ 0 & A & 0 & 0 \\ A & 0 & 0 & -\omega_B \end{pmatrix}, \tag{A16b}$$

or

$$\mathsf{H}'_4 = \begin{pmatrix} \omega_B & 0 & 0 & A \\ 0 & 0 & -A & 0 \\ 0 & -A & 0 & 0 \\ A & 0 & 0 & -\omega_B \end{pmatrix}, \tag{A16c}$$

with $A$ and $B$ given in Table III. The respective time-evolution operators are found to be

$$\mathsf{U}_2(t) = \begin{pmatrix} u_{11} & u_{12} & u_{13} & -u_{14} \\ -u_{12} & u_{22} & u_{23} & u_{13} \\ u_{13} & -u_{23} & u_{22}^* & -u_{12}^* \\ u_{14} & u_{13} & u_{12}^* & u_{11}^* \end{pmatrix}, \tag{A17a}$$

or

$$\mathsf{U}_3(t) = \begin{pmatrix} u_{11} & 0 & 0 & -u_{14} \\ 0 & u_{22} & -u_{23} & 0 \\ 0 & u_{23} & u_{22}^* & 0 \\ u_{14} & 0 & 0 & u_{11}^* \end{pmatrix}, \tag{A17b}$$

or

$$\mathsf{U}_4(t) = \begin{pmatrix} u_{11} & 0 & 0 & u_{14} \\ 0 & u_{22} & -u_{23} & 0 \\ 0 & -u_{23} & u_{22}^* & 0 \\ u_{14} & 0 & 0 & u_{11}^* \end{pmatrix}, \tag{A17c}$$

where the $u_{ij}$ refer to those used for $\mathsf{U}_1(t) = \mathsf{U}(t)$ in Eqs. (A8) but need to be evaluated for the proper values of $A$ and $B$, as listed in Table III. It is straightforward to check that the qubit purity $\mathcal{P}_S(t)$ for $\mathsf{U}_2(t)$, $\mathsf{U}_3(t)$, and $\mathsf{U}_4(t)$ is also given by Eq. (A15), with the $u_{ij}$ modified as just described.

To determine the minimum time for purification, $T_{\min}$, we demand $\dot{\mathcal{P}}_S(t) = 0$ and $\ddot{\mathcal{P}}_S(t) < 0$. Inserting the $u_{ij}$ from Eq. (A14) into Eq. (A15), we find

$$T_{\min} = \frac{\pi}{2\eta_-} \approx \frac{\pi}{2|A|}, \tag{A18}$$

where, in the second step, we have used the approximation of Eq. (A12b). Equation (A18) implies that minimizing the purification time corresponds to maximizing the amplitude of the antidiagonal of $\mathsf{H}'$ in Eq. (A6) for the case $\mathsf{O}_S = \mathsf{O}_B = \mathsf{O}_c = \sigma_1$. For the other cases, the formula for the minimal time $T_{\min}$, cf. Eq. (A18), is identical since $\mathcal{P}_S(t)$ depends only on the moduli of the $u_{ij}$.

Note that $T_{\min}$ is only determined by $\eta_-$, cf. Eq. (A12b), and thus essentially by $|A|$. The latter should be as large as possible for $T_{\min}$ to be minimal. Given a specific choice of $\mathsf{O}_S, \mathsf{O}_B, \mathsf{O}_c \in \{\sigma_1, \sigma_2, \sigma_3\}$, $A$ and $B$ are determined by the resonance condition $\lambda_1 - \lambda_0 = \omega_B$, with $\lambda_0 < \lambda_1$ the eigenvalues of the qubit Hamiltonian $\mathsf{H}_S$, and cannot be chosen at will. Rather, there exist certain combinations of qubit-ancilla interaction and qubit control that maximize $|A|$. This is summarized in Table III, which also indicates $B$ and the respective form of the Hamiltonian, $\mathsf{H}'_i$, $i = 1, \ldots, 4$, cf. Eqs. (A6) and (A16), that generates the dynamics, cf. Eqs. (A7) and (A17).

TABLE III. Summary of the parameters $A$ and $B$ for all interactions $\mathsf{H}_{\text{int}} = J(\mathsf{O}_S \otimes \mathsf{O}_B)$ and local controls $\mathsf{H}_c(t) = \mathcal{E}(t)\mathsf{O}_c$ with $\mathsf{O}_S, \mathsf{O}_B, \mathsf{O}_c \in \{\sigma_1, \sigma_2, \sigma_3\}$. The third column indicates the form ($i$) of the Hamiltonian $\mathsf{H}'_i$, cf. Eqs. (A16). The last column states the minimal time $T_{\min}$, cf. Eq. (A18), for purification of the qubit, evaluated with the same parameters as in Fig. 2.

| $\mathsf{O}_S \otimes \mathsf{O}_B$ | $\mathsf{O}_c$ | Form | $A$ | $B$ | $T_{\min}$ |
|---|---|---|---|---|---|
| $\sigma_1 \otimes \sigma_1$ | $\sigma_1$ | (1) | $J\omega_S/\omega_B$ | $2J\mathcal{E}/\omega_B$ | 46.9 |
| $\sigma_1 \otimes \sigma_1$ | $\sigma_2$ | (3) | $-\mathrm{i}J$ | 0 | 15.7 |
| $\sigma_1 \otimes \sigma_1$ | $\sigma_3$ | (1) | $J$ | 0 | 15.7 |
| $\sigma_1 \otimes \sigma_2$ | $\sigma_1$ | (2) | $\mathrm{i}J\omega_S/\omega_B$ | $-2\mathrm{i}J\mathcal{E}/\omega_B$ | 46.9 |
| $\sigma_1 \otimes \sigma_2$ | $\sigma_2$ | (4) | $J$ | 0 | 15.7 |
| $\sigma_1 \otimes \sigma_2$ | $\sigma_3$ | (2) | $\mathrm{i}J$ | 0 | 15.7 |
| $\sigma_1 \otimes \sigma_3$ | $\sigma_1$ | – | – | – | – |
| $\sigma_1 \otimes \sigma_3$ | $\sigma_2$ | – | – | – | – |
| $\sigma_1 \otimes \sigma_3$ | $\sigma_3$ | – | – | – | – |
| $\sigma_2 \otimes \sigma_1$ | $\sigma_1$ | (3) | $\mathrm{i}J$ | 0 | 15.7 |
| $\sigma_2 \otimes \sigma_1$ | $\sigma_2$ | (1) | $J\omega_S/\omega_B$ | $2J\mathcal{E}/\omega_B$ | 46.9 |
| $\sigma_2 \otimes \sigma_1$ | $\sigma_3$ | (3) | $\mathrm{i}J$ | 0 | 15.7 |
| $\sigma_2 \otimes \sigma_2$ | $\sigma_1$ | (4) | $-J$ | 0 | 15.7 |
| $\sigma_2 \otimes \sigma_2$ | $\sigma_2$ | (2) | $\mathrm{i}J\omega_S/\omega_B$ | $-2\mathrm{i}J\mathcal{E}/\omega_B$ | 46.9 |
| $\sigma_2 \otimes \sigma_2$ | $\sigma_3$ | (4) | $-J$ | 0 | 15.7 |
| $\sigma_2 \otimes \sigma_3$ | $\sigma_1$ | – | – | – | – |
| $\sigma_2 \otimes \sigma_3$ | $\sigma_2$ | – | – | – | – |
| $\sigma_2 \otimes \sigma_3$ | $\sigma_3$ | – | – | – | – |
| $\sigma_3 \otimes \sigma_1$ | $\sigma_1$ | (1) | $-2J\mathcal{E}/\omega_B$ | $J\omega_S/\omega_B$ | 16.7 |
| $\sigma_3 \otimes \sigma_1$ | $\sigma_2$ | (1) | $-2J\mathcal{E}/\omega_B$ | $J\omega_S/\omega_B$ | 16.7 |
| $\sigma_3 \otimes \sigma_1$ | $\sigma_3$ | – | – | – | – |
| $\sigma_3 \otimes \sigma_2$ | $\sigma_1$ | (2) | $-2\mathrm{i}J\mathcal{E}/\omega_B$ | $-\mathrm{i}J\omega_S/\omega_B$ | 16.7 |
| $\sigma_3 \otimes \sigma_2$ | $\sigma_2$ | (2) | $-2\mathrm{i}J\mathcal{E}/\omega_B$ | $-\mathrm{i}J\omega_S/\omega_B$ | 16.7 |
| $\sigma_3 \otimes \sigma_2$ | $\sigma_3$ | – | – | – | – |
| $\sigma_3 \otimes \sigma_3$ | $\sigma_1$ | – | – | – | – |
| $\sigma_3 \otimes \sigma_3$ | $\sigma_2$ | – | – | – | – |
| $\sigma_3 \otimes \sigma_3$ | $\sigma_3$ | – | – | – | – |

The fact that, for all choices of qubit-ancilla interaction and qubit control, only $|A|$ affects the minimal purification time $T_{\min}$ readily explains the analytical and numerical results obtained in Fig. 2 of the main text. Table III also shows that, while purification is possible with several different interactions $\mathsf{H}_{\text{int}} = J(\mathsf{O}_S \otimes \mathsf{O}_B)$, the specific choice of local control $\mathsf{H}_c(t) = \mathcal{E}(t)\mathsf{O}_c$ crucially determines the achievable purification time for that interaction.

### 3. Superpositions of Pauli operators in $\mathsf{H}_{\text{int}}$ and $\mathsf{H}_c(t)$

Next, as a generalization, we drop the restriction to Pauli operators ($\mathsf{O}_S, \mathsf{O}_B, \mathsf{O}_c \in \{\sigma_1, \sigma_2, \sigma_3\}$) and instead allow for

operators of the form $\mathsf{H}_{\rm int} = J(\mathsf{O}_{\rm S}(\varphi_{\rm S},\theta_{\rm S})\otimes\mathsf{O}_{\rm B}(\varphi_{\rm B},\theta_{\rm B}))$ and a local control given by $\mathsf{H}_{\rm c}(t) = \mathcal{E}(t)\mathsf{O}_{\rm c}(\varphi_{\rm c},\theta_{\rm c})$ with

$$\mathsf{O}_k(\varphi_k,\theta_k) = \cos(\varphi_k)\sin(\theta_k)\sigma_1 + \sin(\varphi_k)\sin(\theta_k)\sigma_2 + \cos(\theta_k)\sigma_3, \tag{A19}$$

where the angles are chosen as $\varphi_k \in [0, 2\pi]$ and $\theta_k \in [0,\pi]$ with $k \in \{\mathrm{c},\mathrm{S},\mathrm{B}\}$. Performing the same transformations as described above, i.e., diagonalizing the qubit Hamiltonian $\mathsf{H}_{\rm S}$, one arrives at

$$\mathsf{H}' = \begin{pmatrix} \omega_{\rm B} - B_{\rm c}^{+} & B_{\rm s}^{+}e^{-i\varphi_{\rm B}} & A_{\rm c}^{*} & A_{\rm s}^{*}e^{-i\varphi_{\rm B}} \\ B_{\rm s}^{+}e^{i\varphi_{\rm B}} & B_{\rm c}^{+} & A_{\rm s}^{*}e^{i\varphi_{\rm B}} & -A_{\rm c}^{*} \\ A_{\rm c} & A_{\rm s}e^{-i\varphi_{\rm B}} & -B_{\rm c}^{-} & B_{\rm s}^{-}e^{-i\varphi_{\rm B}} \\ A_{\rm s}e^{i\varphi_{\rm B}} & -A_{\rm c} & B_{\rm s}^{-}e^{i\varphi_{\rm B}} & -\omega_{\rm B} + B_{\rm c}^{-} \end{pmatrix}, \tag{A20}$$

where

$$A_{\rm c} = \bar{A}\cos(\theta_{\rm B}), \tag{A21a}$$

$$A_{\rm s} = \bar{A}\sin(\theta_{\rm B}), \tag{A21b}$$

$$\bar{A} = J\Bigg(\frac{\omega_+ + \omega_-}{2\omega_{\rm B}}\sin(\theta_{\rm S})\cos(\varphi_{\rm c}-\varphi_{\rm S}) - \frac{2\mathcal{E}\cos(\theta_{\rm S})\sin(\theta_{\rm c})}{\omega_{\rm B}} - i\sin(\theta_{\rm S})\sin(\varphi_{\rm c}-\varphi_{\rm S})\Bigg), \tag{A21c}$$

$$B_{\rm c}^{\pm} = J\frac{\cos(\theta_{\rm B})}{\Gamma_{\pm}^{+}}(\cos(\theta_{\rm S})\Gamma_{\pm}^{-} - \xi\omega_{\pm}), \tag{A21d}$$

$$B_{\rm s}^{\pm} = J\frac{\sin(\theta_{\rm B})}{\Gamma_{\pm}^{+}}(\cos(\theta_{\rm S})\Gamma_{\pm}^{-} + \xi\omega_{\pm}), \tag{A21e}$$

$$\xi = 4\mathcal{E}\sin(\theta_{\rm S})\sin(\theta_{\rm c})\cos(\varphi_{\rm c}-\varphi_{\rm S}), \tag{A21f}$$

$$\omega_{\pm} = 2\mathcal{E}\cos(\theta_{\rm c}) + \omega_{\rm S} \pm \omega_{\rm B}, \tag{A21g}$$

$$\Gamma_{\pm}^{+} = 4\mathcal{E}^2\sin^2(\theta_{\rm c}) + \omega_{\pm}^2, \tag{A21h}$$

$$\Gamma_{\pm}^{-} = 4\mathcal{E}^2\sin^2(\theta_{\rm c}) - \omega_{\pm}^2. \tag{A21i}$$

Equation (A20) is a generalization of the Hamiltonians in Eqs. (A6) and (A16), and Eqs. (A21) generalizes the variables accordingly. In particular, $\bar{A}$ is related to $A$, which determines the minimum reset time for Pauli operators and is listed in Table III, by $A = \bar{A}e^{i\varphi_{\rm B}}\sin(\theta_{\rm B})$.

In the general case, Eq. (A19), it is not obvious how to obtain an analytical expression for the time-evolution operator. Nevertheless, generalizing the specific cases presented in Table III provides some insight: According to Table III, purification requires $\mathsf{O}_{\rm B} \neq \sigma_3$; otherwise the Cartan subalgebra is one-dimensional and purity exchange between qubit and ancilla not possible. We therefore expect that a $\sigma_3$ component in $\mathsf{O}_{\rm B}$ will not be helpful for faster purification. To have no $\sigma_3$ component in $\mathsf{O}_{\rm B}$, we have to choose $\theta_{\rm B} = \pi/2$. This implies in particular that the variables $A_{\rm c}$ and $B_{\rm c}^{\pm}$ vanish, cf. Eqs. (A21), which eliminates the additional entries of the generalized Hamiltonian $\mathsf{H}'$ compared to the special cases in Eqs. (A6) and (A16). Furthermore, this choice of $\theta_{\rm B}$ maximizes the magnitude of the antidiagonal, $A_{\rm s} = \bar{A}$. If we assume that, as before, an optimal purification strategy is to maximize the magnitude of the antidiagonal, i.e., $|\bar{A}|$, also with respect to the other angles, then the angle $\varphi_{\rm B}$ cannot be important, since it does not modify the magnitude of any term in Eq. (A20), in other words, $\varphi_{\rm B}$ is only responsible for a complex phase. Hence the task of minimizing the purification time $T_{\rm min}$ in the generalized case reduces to solving a three-angle problem involving $\theta_{\rm c}, \theta_{\rm S}, \varphi_{\rm c} - \varphi_{\rm S}$. Based on this picture, we now conjecture that our result for the case of the Pauli operators ($\mathsf{O}_{\rm S}, \mathsf{O}_{\rm B}, \mathsf{O}_{\rm c} \in \{\sigma_1,\sigma_2,\sigma_3\}$)—namely, that maximal $|A|$, cf. Table III, yields an optimal solution—holds true also for generalized interactions and control operators. This is supported by numerical data, cf. Fig. 4, showing that maximal $1/T_{\rm min}$, hence minimal $T_{\rm min}$, concurs with maximal $\bar{A}$ also for generalized control fields.

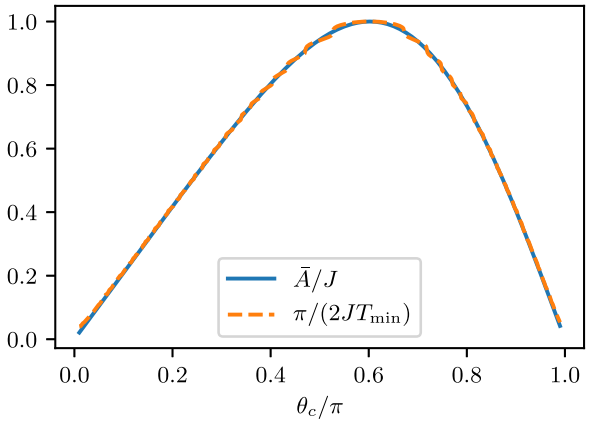


FIG. 4. Behavior of $\bar{A}$ and the numerically obtained inverse purification time $1/T_{\rm min}$ as the control operator is varied via $\theta_c$ from a pure $\sigma_3$ control at $\theta_c = 0$ to $\sigma_1$-control at $\theta_c = \pi/2$ back to a pure $\sigma_3$ control at $\theta_c = \pi$, but with opposite sign. The other angles are chosen such that there is a $\sigma_3 \otimes \sigma_1$ interaction between qubit and ancilla.

Given the importance of $\bar{A}$, respectively $A$, the lack of a physical interpretation of this quantity is dissatisfying. To gain more insight, we revisit Table III, which reveals maximal $A$ as a condition for minimal purification time. Beyond that, given a certain interaction, the purification time is also minimized if the commutator of the control Hamiltonian, $\mathsf{O}_{\rm c}\otimes\mathbb{1}_{\rm B}$, and the interaction Hamiltonian, $\mathsf{H}_{\rm int} = J(\mathsf{O}_{\rm S}\otimes\mathsf{O}_{\rm B})$, has maximum norm. The latter information can be compressed into the quantity $C = \frac{1}{2\sqrt{2}}\|[\mathsf{O}_{\rm S},\mathsf{O}_{\rm c}]\|$, which allows for a physical interpretation: One can show that the norm of the commutator of $\mathsf{O}_{\rm c}$ and $\mathsf{O}_{\rm S}$ sets an upper limit to the energy (or, more specifically, heat) exchange between the qubit and ancilla:

$$|\dot{Q}| = \mathrm{tr}(\dot{\rho}_{\rm S}\mathsf{H}_{\rm S}) \leqslant \sqrt{2}J(\mathcal{E}\|[\mathsf{O}_{\rm S},\mathsf{O}_{\rm c}]\| + \frac{\omega_{\rm S}}{2}\|[\sigma_3,\mathsf{O}_{\rm S}]\|). \tag{A22}$$

One may now wonder whether $C$, relevant for the rate of heat exchange, is related to $\bar{A}$, whose maximum is a condition for minimal purification time.

To check whether maximizing $|\bar{A}|$ corresponds to the same purification strategy as maximizing $C$, we evaluate the two quantities for different interactions and control fields and depict the corresponding values in Fig. 5. The results show that although the two quantities behave very similarly, they only

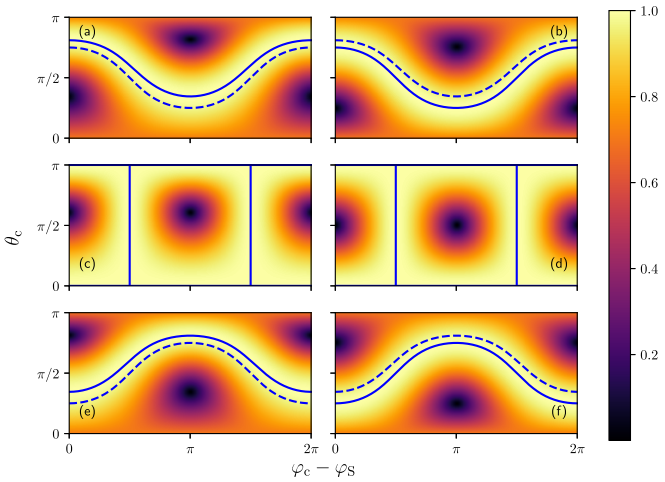


FIG. 5. The figure shows the values of $|\bar{A}|$ (left column) and $C$ (right column) for different interactions and control fields. These are determined by $\theta_S = \pi/4$ in (a), (b); $\theta_S = \pi/2$ in (c), (d); and $\theta_S = 3\pi/2$ in (e), (f); and the axes represent the angles $\theta_c$ and $\varphi_c - \varphi_S$. The solid blue line indicates the maximum value of 1 for the respective quantity, $|\bar{A}|$ or $|C|$, while the dashed line depicts the maximum value for the other quantity ($|C|$ or $|\bar{A}|$) to ease comparison. Except for (c) and (d), the lines do not coincide and therefore the limit on the energy exchange between qubit and ancilla, which is determined by $C$, cf. Eq. (A22), does not fully explain the physical role of $\bar{A}$.

coincide for certain cases, namely, those indicated by the vertical lines in Figs. 5(c) and 5(d). Incidentally, these are exactly the pure Pauli operator choices for which the global minimum of the purification time can be realized, cf. $T_{\min} = \pi/(2J)$ corresponding to $T_{\min}^{(1)}$ in the main text and resulting in the value of 15.7 in Table III. In these cases, both $C$ and $|\bar{A}|$ are maximal. This underpins our claim of having identified the globally minimal purification time. On the other hand, the different behavior of $C$ and $|\bar{A}|$ as a function of the angles in general indicates that the heat exchange argument made in Eq. (A22) alone cannot fully explain the significance of $\bar{A}$. This requires further investigation, which will be the subject of future research.

## APPENDIX B: MAXIMALLY ACHIEVABLE QUBIT PURITY EMPLOYING QUDIT ANCILLAS

In this Appendix, we turn toward ancillas with Hilbert space dimension $d_B > 2$. While we discuss the impact of such higher dimensional ancillas on the reset time in Sec III, here we entirely focus on their impact on the maximal achievable qubit purity, i.e., on the motivation and proof of proposition 1. To keep the results as general as possible, we do not assume any specific Hamiltonian for the bipartite system of qubit and ancilla.

As before, we assume an initially separable state of qubit and ancilla, $\rho = \rho_S \otimes \rho_B$, where the ancilla Hilbert space has dimension $d_B$. We seek to find those unitary transformations $\mathsf{U} \in \mathrm{SU}(2d_B)$ such that the purity of the time-evolved qubit,

$$\rho_S' = \mathrm{tr}_B\{\mathsf{U}\rho\mathsf{U}^\dagger\} = \mathcal{D}_{\rho_B}[\rho_S], \tag{B1}$$

is maximized—irrespective of the Hamiltonian and control fields that generate those unitaries. First, we demand the state $\rho'$ yielding maximal purity to be separable, $\rho' = \rho_S' \otimes \rho_B'$. Since the ultimate goal is to purify the qubit, which includes erasing all correlations with the ancilla, it is natural to consider a separable target state.

Next, we write the initial states of qubit and ancilla in the respective eigenbases, $\{|s_1\rangle, |s_2\rangle\}$ and $\{|b_1\rangle, \ldots, |b_{d_B}\rangle\}$,

$$\rho_S = \sum_{i=1}^{2} s_i |s_i\rangle\langle s_i|, \quad \rho_B = \sum_{j=1}^{d_B} b_j |b_j\rangle\langle b_j|. \tag{B2}$$

The eigenvalues of $\rho_S$ and $\rho_B$ obey $0 \leqslant s_1, s_2 \leqslant 1$ and $0 \leqslant b_1, \ldots, b_{d_B} \leqslant 1$ with $s_1 + s_2 = 1$ and $\sum_{j=1}^{d_B} b_j = 1$. Thus, the joint initial state reads

$$\rho = \sum_{i=1}^{2}\sum_{j=1}^{d_B} \lambda_{i,j} |s_i\rangle\langle s_i| \otimes |b_j\rangle\langle b_j|, \quad \lambda_{i,j} = s_i b_j. \tag{B3}$$

Since we demand the final state to be separable as well, we can write, using prime for all transformed quantities,

$$\rho' = \sum_{i=1}^{2}\sum_{j=1}^{d_B} \lambda'_{i,j} |s'_i\rangle\langle s'_i| \otimes |b'_j\rangle\langle b'_j|. \tag{B4}$$

Due to the unitary nature of the transformation, the spectra $\{\lambda_{i,j}\}$ and $\{\lambda'_{i,j}\}$ of the joint states $\rho$ and $\rho'$ are identical. However, $\mathsf{U}$ allows for spectral reordering, which is what ultimately allows purification of the qubit. Due to the separability of $\rho'$, the qubit purity becomes

$$\mathcal{P}_S = \mathrm{tr}\{\rho_S'^2\} = \sum_{i=1}^{2} s_i'^2, \quad s_i' = \sum_{j=1}^{d_B} \lambda'_{i,j}. \tag{B5}$$

We can interpret the elements of the qubit spectrum after the reset, $\{s_1', s_2'\}$, as entries of a vector, $\boldsymbol{s'} = (s_1', s_2')^\top$. By means of Karamata's inequality and using the concept of majorization, we can construct an operation $\mathsf{U}$ that yields maximal $\mathcal{P}_S$.

*Definition (majorization).* Let $\boldsymbol{a}, \boldsymbol{b} \in \mathbb{R}^d$, $d \in \mathbb{N}$, and let $\boldsymbol{a}^\downarrow, \boldsymbol{b}^\downarrow$ be reshuffled vectors $\boldsymbol{a}, \boldsymbol{b}$ with their elements sorted in descending order. The vector $\boldsymbol{a}$ majorizes the vector $\boldsymbol{b}$, i.e., $\boldsymbol{a} \succ \boldsymbol{b}$, if $\sum_{n=1}^{d} a_n = \sum_{n=1}^{d} b_n$ and $\sum_{n=1}^{k} a_n^\downarrow \geqslant \sum_{n=1}^{k} b_n^\downarrow$ for all $k = 1, \ldots, d$.

*Theorem 3 (Karamata's inequality).* Let $I$ be an interval of the real line, $I \subset \mathbb{R}$, and $f : I \to \mathbb{R}$ a convex function. If $\boldsymbol{a} \succ \boldsymbol{b}$ for $\boldsymbol{a}, \boldsymbol{b} \in I^d$, $d \in \mathbb{N}$, then

$$\sum_{n=1}^{d} f(a_i) \geqslant \sum_{n=1}^{d} f(b_i).$$

If $f$ is strictly convex then $\sum_{n=1}^{d} f(a_i) = \sum_{n=1}^{d} f(b_i)$ iff $\boldsymbol{a} = \boldsymbol{b}$.

Taking into account the strict convexity of the function $f(x) = x^2$, we know that, if $\boldsymbol{s'}^* \succ \boldsymbol{s'}$, then

$$\mathcal{P}_S(\boldsymbol{s'}^*) = \sum_i f(s_i'^*) \geqslant \sum_i f(s_i') = \mathcal{P}_S(\boldsymbol{s'}). \tag{B6}$$

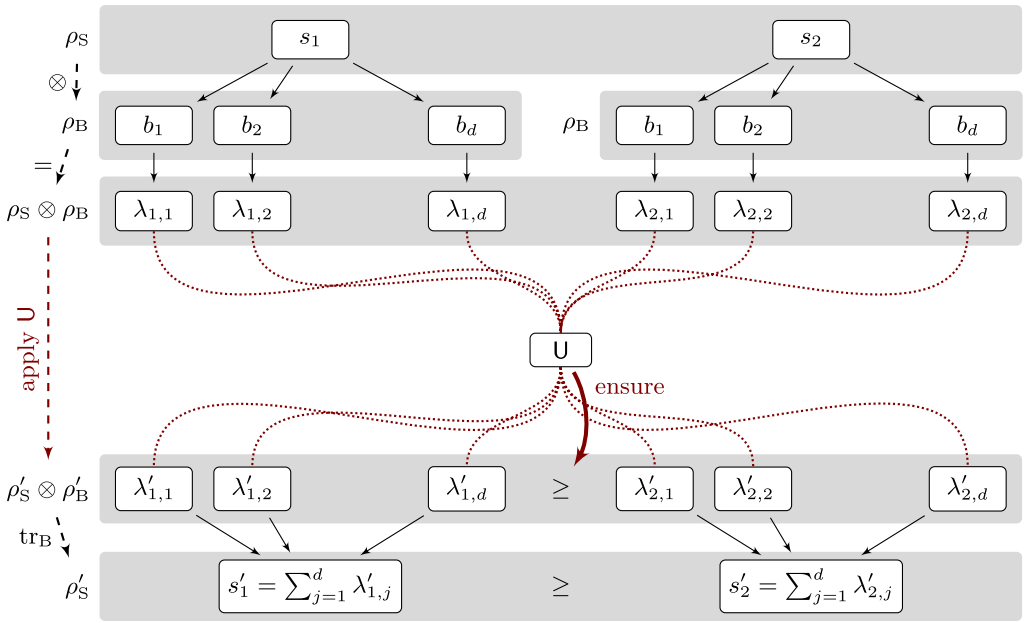


FIG. 6. Sketch of the reshuffling operation on the joint qubit ancilla spectrum that maximizes the qubit purity.

Thus, for maximal qubit purification, we have to find a vector $\boldsymbol{s}'^*$ that majorizes all other vectors accessible via spectral reshuffling from $\{\lambda_{i,j}\}$ to $\{\lambda'_{i,j}\}$. With the constraint $s'^*_1 + s'^*_2 = 1$ for a qubit, majorization of $\boldsymbol{s}'^*$ implies, without loss of generality, maximization of $s'^*_1 = \sum_{j=1}^{d_B} \lambda'_{1,j}$, cf. Eqs. (B5). Hence, the unitary transformation $\mathsf{U} \in \mathrm{SU}(2d_B)$ needs to reshuffle the $2d_B$ elements from the initial set $\{\lambda_{1,1}, \ldots, \lambda_{1,d_B}, \lambda_{2,1}, \ldots, \lambda_{2,d_B}\}$, which can be in any order, such that the first half of the reordered set $\{\lambda'_{1,1}, \ldots, \lambda'_{1,d_B}, \lambda'_{2,1}, \ldots, \lambda'_{2,d_B}\}$ contains the $d_B$ largest eigenvalues and the second half the remaining ones. The reshuffling is sketched in Fig. 6. Karamata's inequality then guarantees that this gives the largest achievable qubit purity.

A possible choice for $\mathsf{U}$ is given by the permutation matrix that transforms the vector $\boldsymbol{\lambda} = (\lambda_{1,1}, \ldots, \lambda_{1,d_B}, \lambda_{2,1}, \ldots, \lambda_{2,d_B})^\top$ into the vector $\boldsymbol{\lambda}' = (\lambda'_{1,1}, \ldots, \lambda'_{1,d_B}, \lambda'_{2,1}, \ldots, \lambda'_{2,d_B})^\top$. Note that $\mathsf{U}$ is not unique since, for instance, any local operation on either the qubit or the ancilla leaves the qubit purity invariant.

The protocol described so far can easily be generalized to arbitrary qudit-qudit systems. One only needs to ensure that the unitary $\mathsf{U}$ reshuffles all elements from $\{\lambda_{i,j}\}$ such that the vector $\boldsymbol{s}'^* = (s'^*_1, s'^*_2, \ldots)^\top$ majorizes all other accessible vectors.

The above results have an interesting implication. Let us assume that at least half (rounded up) of the initial eigenvalues $\{b_1, \ldots, b_{d_B}\}$ of $\rho_B$ are zero. As a consequence, at least half of the eigenvalues $\{\lambda_{i,j}\}$ of the initial qubit-ancilla state will be zero. Assuming full unitary controllability, these eigenvalues can be reshuffled such that the first half, namely $\lambda'_{1,j}$ with $j = 1, \ldots, d_B$, contains all nonzero eigenvalues whereas the other half, $\lambda'_{2,j}$ with $j = 1, \ldots, d_B$, contains only zeros. Equations (B5) then imply $s'_1 = 1$ and $s'_2 = 0$, i.e., we obtain a pure state $\mathcal{P}_S = 1$—independently of the initial qubit state $\rho_S$ and despite the fact that $\rho_B$ is mixed. For ancillas with Hilbert space dimension larger than two, it is therefore possible to purify the qubit beyond a simple swap of purities.

We can generalize our observation to arbitrary Hilbert space dimensions of system and ancilla. The following proposition reveals the relation between Hilbert space dimensions and achievable purity.

*Proposition.* Let $\mathcal{H}_S$ and $\mathcal{H}_B$ be Hilbert spaces with dimension $d_S$ and $d_B$, respectively, and $\mathfrak{L}_{\mathcal{H}_S}$ and $\mathfrak{L}_{\mathcal{H}_B}$ their corresponding Liouville spaces. Let $\rho_B \in \mathfrak{L}_{\mathcal{H}_B}$ be a density matrix with at least $\lceil d_B(d_S - 1)/d_S \rceil$ eigenvalues below $\epsilon/[2d_B(d_S - 1)]$ with small $\epsilon > 0$, where $\lceil \cdot \rceil$ denotes the ceiling function. Then, for all density matrices $\rho_S \in \mathfrak{L}_{\mathcal{H}_S}$, there exists a $\mathsf{U} \in \mathrm{SU}(d_S d_B)$ such that

$$1 - \mathrm{tr}\{\rho'^2_S\} \leqslant \epsilon, \quad \rho'_S = \mathrm{tr}_B\{\mathsf{U}(\rho_S \otimes \rho_B)\mathsf{U}^\dagger\}, \tag{B7}$$

i.e., the purity of $\rho'_S$ gets $\epsilon$-close to unity.

*Proof.* Let $\{\lambda_{i,j}\}$ and $\{\lambda'_{i,j}\}$ be the spectra of the states $\rho = \rho_S \otimes \rho_B$ and $\rho' = \mathsf{U}\rho\mathsf{U}^\dagger = \rho'_S \otimes \rho'_B$, defined in the same way as in Eqs. (B3) and (B4). Since $\mathsf{U}$ is unitary, these spectra are identical up to reshuffling. The purity of $\rho'_S$ reads $\mathcal{P}_S = \mathrm{tr}\{\rho'^2_S\} = \sum_{i=1}^{d_S} s'^2_i$ with $s'_i = \sum_{j=1}^{d_B} \lambda'_{i,j}$. Exploiting unit trace, $\sum_{i=1}^{d_S} s'_i = 1$, we can rewrite the purity as $\mathcal{P}_S = 1 + 2\sum_{i=2}^{d_S} s'_i(s'_i - 1)$, from which we deduce that

$$1 - \mathcal{P}_S \leqslant \epsilon \quad \Leftrightarrow \quad \sum_{i=2}^{d_S} s'_i(s'_i - 1) \leqslant \frac{\epsilon}{2}. \tag{B8}$$

Since $s'_i \in [0, 1]$, $i = 1, \ldots, d_S$, one option to ensure the latter inequality is

$$\sum_{i=2}^{d_S} s'_i \leqslant \frac{\epsilon}{2}, \tag{B9}$$

since $\sum_{i=2}^{d_S} s_i'(s_i'-1) \leqslant \sum_{i=2}^{d_S} s_i'$. We now assume that $n < d_B$ eigenvalues of $\rho_B$ are below some small $\delta > 0$. Thus, we know that $d_S n$ eigenvalues in $\{\lambda_{i,j}\}$ will be below $\delta$. If $d_S n \geqslant d_B(d_S-1)$, which implies $n \geqslant d_B(d_S-1)/d_S$, then we can reshuffle $\{\lambda_{i,j}\}$ into $\{\lambda'_{i,j}\}$ in such a way that all elements $\lambda'_{i,j} \leqslant \delta$ for $i = 2,\ldots,d_S$ and $j = 1,\ldots,d_B$. Hence, we find $s_i' = \sum_{j=1}^{d_B} \lambda'_{i,j} \leqslant \delta d_B$, $i = 2,\ldots,d_S$. Plugging this into Eq. (B9), we obtain

$$\sum_{i=2}^{d_S} s_i' \leqslant (d_S-1) d_B \delta \leqslant \frac{\epsilon}{2}. \tag{B10}$$

This can be guaranteed if $\delta \leqslant \epsilon/[2d_B(d_S-1)]$ and the proposition follows. ■


[1] D. P. DiVincenzo, The physical implementation of quantum computation, Fortschr. Phys. **48**, 771 (2000).

[2] M. A. Nielsen and I. L. Chuang, *Quantum Computation and Quantum Information* (Cambridge University Press, Cambridge, 2000).

[3] D. Ristè, J. G. van Leeuwen, H.-S. Ku, K. W. Lehnert, and L. DiCarlo, Initialization by Measurement of a Superconducting Quantum Bit Circuit, Phys. Rev. Lett. **109**, 050507 (2012).

[4] J. E. Johnson, C. Macklin, D. H. Slichter, R. Vijay, E. B. Weingarten, J. Clarke, and I. Siddiqi, Heralded State Preparation in a Superconducting Qubit, Phys. Rev. Lett. **109**, 050506 (2012).

[5] P. O. Boykin, T. Mor, V. Roychowdhury, F. Vatan, and R. Vrijen, Algorithmic cooling and scalable NMR quantum computers, Proc. Natl. Acad. Sci. USA **99**, 3388 (2002).

[6] D. Basilewitsch, R. Schmidt, D. Sugny, S. Maniscalco, and C. P. Koch, Beating the limits with initial correlations, New J. Phys. **19**, 113042 (2017).

[7] K. Geerlings, Z. Leghtas, I. M. Pop, S. Shankar, L. Frunzio, R. J. Schoelkopf, M. Mirrahimi, and M. H. Devoret, Demonstrating a Driven Reset Protocol for a Superconducting Qubit, Phys. Rev. Lett. **110**, 120501 (2013).

[8] P. Magnard, P. Kurpiers, B. Royer, T. Walter, J.-C. Besse, S. Gasparinetti, M. Pechal, J. Heinsoo, S. Storz, A. Blais, and A. Wallraff, Fast and Unconditional All-Microwave Reset of a Superconducting Qubit, Phys. Rev. Lett. **121**, 060502 (2018).

[9] D. J. Egger, M. Werninghaus, M. Ganzhorn, G. Salis, A. Fuhrer, P. Müller, and S. Filipp, Pulsed Reset Protocol for Fixed-Frequency Superconducting Qubits, Phys. Rev. Appl. **10**, 044030 (2018).

[10] S. Deffner and S. Campbell, Quantum speed limits: From Heisenberg's uncertainty principle to optimal quantum control, J. Phys. A: Math. Theor. **50**, 453001 (2017).

[11] M. Kjaergaard, M. E. Schwartz, J. Braumüller, P. Krantz, J. I.-J. Wang, S. Gustavsson, and W. D. Oliver, Superconducting qubits: Current state of play, Annu. Rev. Condens. Matter Phys. **11**, 369 (2020).

[12] N. Khaneja, R. Brockett, and S. J. Glaser, Time optimal control in spin systems, Phys. Rev. A **63**, 032308 (2001).

[13] R. Romano and D. D'Alessandro, Incoherent control and entanglement for two-dimensional coupled systems, Phys. Rev. A **73**, 022323 (2006).

[14] R. Romano, Relaxation to equilibrium driven via indirect control in Markovian dynamics, Phys. Rev. A **76**, 052115 (2007).

[15] R. Romano, Resonant purification of mixed states for closed and open quantum systems, Phys. Rev. A **75**, 024301 (2007).

[16] D. D'Alessandro, *Introduction to Quantum Control and Dynamics* (Chapman and Hall, Boca Raton, 2008).

[17] R. Gilmore, *Lie Groups, Lie Algebras and Some of Their Applications* (Wiley-Interscience, New York, 1974).

[18] S. J. Glaser, U. Boscain, T. Calarco, C. P. Koch, W. Köckenberger, R. Kosloff, I. Kuprov, B. Luy, S. Schirmer, T. Schulte-Herbrüggen, D. Sugny, and F. K. Wilhelm, Training Schrödinger's cat: Quantum optimal control, Eur. Phys. J. D **69**, 279 (2015).

[19] J. Fischer, D. Basilewitsch, C. P. Koch, and D. Sugny, Time-optimal control of the purification of a qubit in contact with a structured environment, Phys. Rev. A **99**, 033410 (2019).

[20] Y. Shalibo, Y. Rofe, D. Shwa, F. Zeides, M. Neeley, J. M. Martinis, and N. Katz, Lifetime and Coherence of Two-Level Defects in a Josephson Junction, Phys. Rev. Lett. **105**, 177001 (2010).

[21] D. M. Reich, N. Katz, and C. P. Koch, Exploiting non-Markovianity for quantum control, Sci. Rep. **5**, 12430 (2015).

[22] F. Ticozzi and L. Viola, Quantum resources for purification and cooling: Fundamental limits and opportunities, Sci. Rep. **4**, 5192 (2014).

[23] F. Ticozzi and L. Viola, Quantum and classical resources for unitary design of open-system evolutions, Quantum Sci. Technol. **2**, 034001 (2017).

[24] H.-K. Lau and A. A. Clerk, High-fidelity bosonic quantum state transfer using imperfect transducers and interference, npj Quantum Inf. **5**, 31 (2019).

[25] J. Zhang, J. Vala, S. Sastry, and K. B. Whaley, Geometric theory of nonlocal two-qubit operations, Phys. Rev. A **67**, 042313 (2003).

[26] A map is called unital if it maps the identity onto itself.

[27] S. Lorenzo, F. Plastina, and M. Paternostro, Geometrical characterization of non-Markovianity, Phys. Rev. A **88**, 020102(R) (2013).

[28] Strictly speaking, nonunitality of $\mathcal{D}_{\rho_B(0)}$ also requires an ancilla initial state $\rho_B \neq \mathbb{1}_B/2$, but this is irrelevant since a totally mixed state of the ancilla would not allow purification in the first place.

[29] Note that it is sufficient to consider constant couplings $J$ since time-optimal protocols will require $J(t)$ to take its maximum value [6].

[30] Note that the equality of $\dim\{\mathfrak{a}\}$ and $N_c$ holds for Hamiltonians of the form Eq. (6) but not in general.

[31] Note that $N_c \leqslant 2$ for Hamiltonian Eq. (6) but this is sufficient for purification together with the assumption of a thermal initial ancilla state, i.e., $\gamma_B = 0$. Then $\gamma_B'$ has to be zero as well since the local operations $\mathsf{k}_B'$ for Hamiltonian Eq. (6) are generated only by $\mathbb{1}_S \otimes \mathbb{1}_B$ and $\mathbb{1}_S \otimes \sigma_3$ which do not change the ancilla coherence. $\gamma_B' = 0$ implies nonunitality according to Eq. (5).

[32] A. Konnov and V. F. Krotov, On global methods of successive improvement of controlled processes, Autom. Remote Control **60**, 1427 (1999).

[33] D. M. Reich, M. Ndong, and C. P. Koch, Monotonically convergent optimization in quantum control using Krotov's method, J. Chem. Phys. **136**, 104103 (2012).

[34] Note that for the optimizations in Fig. 2(b), a second control, coupling to $\mathsf{O}_c = \sigma_1$, has been utilized, since $\mathsf{O}_c = \sigma_3$ alone is not sufficient for modifying the qubit coherence.

[35] C. Rigetti, A. Blais, and M. Devoret, Protocol for Universal Gates in Optimally Biased Superconducting Qubits, Phys. Rev. Lett. **94**, 240502 (2005).

[36] C. Rigetti and M. Devoret, Fully microwave-tunable universal gates in superconducting qubits with linear couplings and fixed transition frequencies, Phys. Rev. B **81**, 134507 (2010).

[37] L.-A. Wu, D. Segal, and P. Brumer, No-go theorem for ground state cooling given initial system-thermal bath factorization, Sci. Rep. **3**, 1824 (2013).